8-4-2021

Methane Emissions from Stormwater Ponds

Brianna Pollard
brp7104@rit.edu

RIT

Methane Emissions from Stormwater Ponds

by Brianna Pollard

A Thesis Submitted in Partial Fulfillment of the Requirements for the Degree of Master of Science in Environmental Science

Gosnell School of Life Sciences
College of Science
Environmental Science Program

Rochester Institute of Technology
Rochester, NY
August 4th, 2021

Committee Approval:

Carmody McCalley, PhD — Date
Committee Member, Thesis Advisor

Anna Christina Tyler, PhD — Date
Committee Member

Ruth Varner, PhD — Date
Committee Member

Nathan Eddingsaas, PhD — Date
Committee Member

Table of Contents

Acknowledgements

I would like to extend my deepest thanks and gratitude to my advisor, Dr. Carrie McCalley. This project would not have been possible without her guidance and brainpower. I would also like to thank the members of my committee. Thank you to Dr. Christy Tyler for being a tremendous help throughout my years in the aquatic ecology lab group, to Dr. Ruth Varner for allowing me to run samples at UNH, and to Dr. Nathan Eddingsaas for helping me through NMR analysis.

I also give my gratitude to the RIT College of Science, who provided funding and resources, and to the Town of Henrietta for allowing me to sample from Town stormwater ponds. Thank you to Jesse Gilman for helping out on the ponds, but most importantly, for cutting the Styrofoam because that noise was intolerable. Thank you to Evan Squier for helping and providing company even when the weather was miserable. My deepest gratitude goes out to all members of the aquatic ecology lab group for keeping me a little saner throughout my time in the lab. And lastly, I would like to thank my friend Shannon McHugh for letting me dwell with her these past years and for putting up with my bubble trap nonsense. Sincerest thanks to all!

List of Tables and Figures

Abstract

Methane (CH_4) is a powerful greenhouse gas that has a global warming potential 28 times larger than carbon dioxide (CO_2) on a 100-year horizon. Methane emissions from inland freshwater sources are not as well understood as those from other sources; however, current estimates suggest that they account for a significant portion of global CH_4 emissions. Emissions from inland waters are difficult to measure due to their high spatiotemporal variability, leading to high levels of uncertainty and a need for more CH_4 flux data from these freshwater systems. Increased runoff associated with urbanization has led to construction of man-made inland waters called stormwater ponds. Methane emission estimates for stormwater ponds are very limited and, therefore, are typically not included in the global CH_4 budget. In order to reduce uncertainty in the global CH_4 budget and to understand how urbanization more fully impacts greenhouse gas emissions, there is a need to characterize CH_4 emissions from these ecosystems. The objective of this study was to accurately quantify CH_4 emissions from stormwater ponds in Rochester, NY. I hypothesized that high nutrient and sediment inputs in stormwater ponds would support high rates of methanogenesis. Bubble traps were used to quantify ebullitive CH_4 flux and floating chambers with shields were used to quantify diffusive CH_4 flux. The combined ebullitive and diffusive CH_4 flux from June to October averaged 268 mg CH_4 m^{-2} d^{-1} of which 96% was from ebullition and there was significant variability both seasonally and amongst ponds. July had the greatest ebullitive flux at 386 mg CH_4 m^{-2} d^{-1} and ebullitive flux varied by 27 times from the highest CH_4 emitting pond to the lowest. In addition to temperature driven seasonal patterns, depth and nutrient status were drivers of CH_4 emissions from stormwater ponds.

1.0 Introduction

1.1 Stormwater ponds

In 1950, 30% of the world's population lived in urban areas. This percentage rose to 54% in 2014 and is projected to reach 66% by 2050 (Bocquier, 2005). This rapid urbanization has led to increased development in and around cities, resulting in an increase in flooding and a decrease in water quality due to amplified runoff. The Clean Water Act was amended in 1987 to address the issue of reduced water quality generated by stormwater runoff. This amendment made it mandatory for municipalities to control the discharge of pollutants using management practices, control techniques, and system design and engineering methods (EPA, 1987). One control technique widely implemented and seen throughout the urban landscape today is the construction of stormwater ponds (Saulnier-Talbot & Lavoie, 2018). These stormwater ponds are designed to mitigate flooding and limit water quality degradation associated with stormwater runoff (EPA, 2009).

Stormwater ponds are helpful in reducing runoff volume and mitigating water quality degradation; however, a less studied potential consequence of stormwater ponds is greenhouse gas emissions. Greenhouse gases in the atmosphere induce a global warming effect that has increased global atmospheric temperatures by 1°C since the pre-industrial age. Increasing global temperatures are expected to negatively impact human health, food security, water supply, and economic growth (IPCC, 2018). To date, few studies have evaluated carbon dioxide (CO_2), nitrous oxide (N_2O) or methane (CH_4) emissions from stormwater ponds, creating a lack of data on greenhouse gas emissions from these ecosystems (Blaszczak et al., 2018; Herrero Ortega, Romero González-Quijano, Casper, Singer, & Gessner, 2019; Kavehei, Jenkins, Adame, & Lemckert, 2018; Moore & Hunt, 2013; van Bergen et al., 2019). In order to better understand

how stormwater ponds are affecting global warming, more studies on greenhouse gas emissions are needed.

1.2 Methane emissions from freshwater ecosystems

Methane is an important greenhouse gas, contributing significantly to global warming, making it imperative to understand where CH_4 emissions are coming from and how much is being emitted from individual sources and regions. In freshwater ecosystems, water-saturated sediments often support high rates of methanogenesis (Bastviken, 2009), resulting in global estimates of CH_4 release of 103 Tg CH_4 yr^{-1} (Bastviken, Tranvik, Downing, Crill, & Enrich-Prast, 2011). Sources of CH_4 in the atmosphere can be determined using either bottom-up or top-down modeling approaches, where bottom-up models scale CH_4 emission sources based on flux and land-cover data whereas top-down approaches work backwards from atmospheric CH_4 observations to determine sources of CH_4. Kirschke et al. (2013) showed that models using bottom-up approaches for determining global estimations of CH_4 emissions have high uncertainty and overestimate natural emissions. Similarly, Saunois et al. (2016) emphasized that bottom-up modeling methods do not match up with the latitudinal data from top-down emissions. Over the 2003-2012 decade, bottom-up methods indicated that the global CH_4 emission rate was 384 Tg CH_4 yr^{-1}, whereas top-down methods indicated a rate of only 231 Tg CH_4 yr^{-1}. Part of this identified uncertainty comes from the limited data on the interannual and decadal changes in CH_4 flux from freshwater ecosystems. Therefore, increased field studies quantifying CH_4 flux from freshwater ecosystems is crucial in mitigating uncertainty in global CH_4 budgets. Additionally, $\delta^{13}C$-CH_4 can be used when modelling global CH_4 emissions since $\delta^{13}C$-CH_4 provides insight to sources of emissions (Hein, Crutzen, & Heimann, 1997). Thus, investigating isotope ratios in

stormwater ponds will help fill the gap in knowledge on CH_4 flux pathway and formation dynamics, as well as provide missing information for the global CH_4 budget.

Methane is produced in aquatic ecosystems by the microbial process of methanogenesis, an important terminal step in anoxic organic matter (OM) decomposition. This process is carried out by chemoautotrophic archaebacteria called methanogens, that use hydrogen (H_2) and carbon dioxide (CO_2), or acetate (CH_3OO^-), to produce CH_4 (Figure 1). Other low molecular weight substrates can be used by methanogens to produce CH_4, however, H_2/CO_2 and acetate tend to be the most commonly used substrate. Carbon isotopes ($\delta^{13}C$) can be used to gain insight into the relative role of acetate fermentation (acetoclastic) and CO_2 reduction (hydrogenotrophic) in CH_4 production within an ecosystem (Barker, 1936; Takai, 1970). Acetoclastic production results in higher $\delta^{13}C$ abundance compared to hydrogenotrophic production (Chanton, Chaser, Glasser, & Siegel, 2005).

Methane produced in the sediment can reach the atmosphere through three different pathways: diffusive, plant-mediated and ebullitive flux (Figure 1). Diffusive flux involves molecular diffusion at the sediment-water interface, followed by CH_4 transport to the water column by diffusion or advection. Once CH_4 reaches the water-air interface, CH_4 diffuses into the atmosphere. Similar to how plants can transport O_2 from the atmosphere to the soil, plants can transport CH_4 from the sediment to the atmosphere; this is plant-mediated flux (Bastviken, 2009). In stormwater ponds, plant-mediated flux is assumed to be insignificant since there is very little emergent vegetation. Methane is largely insoluble in water therefore CH_4 bubbles form in the sediment (Poissant et al., 2007). Once they reach a concentration in which the partial pressure of CH_4 exceeds the in-situ pressure, bubbles are rapidly released and travel through the water column and into the atmosphere. This episodic flux is called ebullition and in open freshwater, it

is the dominant CH_4 flux pathway, making it very important to quantify as accurately as possible (Casper, Maberly, Hall, & Finlay, 2000).

Methane produced in anaerobic sediments can be by consumed through the process of methanotrophy, also known as CH_4 oxidation, which is carried out by microorganisms in oxic conditions that oxidize CH_4 to CO_2 (Whalen, 2005, Figure 1). In aquatic ecosystems, CH_4 oxidation often occurs in the water column and in areas of oxygenated sediment, such as in sediment oxygenated by root transport (Bastviken, 2009). Methanotrophy therefore has the potential to limit CH_4 emissions through the consumption of produced CH_4, with estimates of a 85% reduction in diffusive CH_4 flux due to CH_4 oxidation in one aquatic ecosystem (Guérin & Abril, 2007). Isotopes provide information about CH_4 transport and oxidation. During CH_4 oxidation, methanotrophs have a preference for the consumption of lighter isotopes, resulting in the enrichment of the remaining CH_4. Therefore, CH_4 from diffusive flux have a higher $\delta^{13}C$, due to interaction with methanotrophs within the water column (Chanton et al., 2005). Conversely, since ebullitive CH_4 flux bypasses methanotrophs in the water column, ebullitive CH_4 emissions will have a lighter isotopic signature than diffusive flux, with the magnitude of this difference indicative of rates of CH_4 oxidation (Chanton & Martens, 1988).

1.3 Controls on CH_4 emissions

There are numerous known controls on CH_4 emissions in aquatic freshwater ecosystems. Changes in temperature strongly affect CH_4 production. Methanogenesis peaks at 30 to 40 °C and is lowest at 5 °C (Boon & Mitchell, 1995). Likewise, a 10 °C increase has been shown to increase CH_4 production by 4x (Bastviken, 2009). This results in seasonal variations in CH_4 flux (Boon & Mitchell, 1995). Temperature also affects available substrates, at low temperatures,

acetate formation is favored over propionate formation during fermentation, resulting in a high availability of acetate for methanogens. In these conditions methanogens will rely more heavily on acetate than on CO_2/H_2 (Conrad, 2002). The temperature of the porewater within the sediment also affects ebullitive flux; with higher temperatures decreasing CH_4 solubility, resulting in an increase in ebullition. This can contribute to seasonal variation in ebullitive flux, with high temperature increasing both the activity of methanogens and the rate of ebullition (Bastviken, 2009; Boon & Mitchell, 1995; J. P. Chanton, Martens, & Kelley, 1989). Stormwater ponds are frequently impacted by thermal pollution therefore temperature is likely to play an important role in the magnitude of CH_4 emissions. Thermal pollution in stormwater ponds occurs when runoff picks up thermal energy as it travels over low albedo, urban surfaces. Increases in impervious surface cover from 20% to 50% can yield a 3 °C increase in runoff temperature (Sabouri, Gharabaghi, Mahboubi, & McBean, 2013). Additionally, runoff storage within a pond can give rise to increased water temperature. Measurements have shown that outflow of runoff from a stormwater pond was 1.2 °C higher than the inflow, thus adding further thermal energy to the water within the stormwater pond (Herb, Mohseni, & Stefan, 2009).

Pressure also has a large effect on ebullitive flux; the greater the pressure applied to the sediment, the smaller the ebullitive flux and vice versa. Rates of ebullition should therefore increase as water depth decreases due to decreased hydrostatic pressure (Chanton et al., 1989; Holgerson & Raymond, 2016). Shallow lakes and ponds, such as stormwater ponds, often have a large ebullitive flux (Holgerson & Raymond, 2016; Natchimuthu, Panneer Selvam, & Bastviken, 2014; van Bergen et al., 2019). For example, Casper et al. (2000) found that ebullitive flux accounted for 96% of CH_4 emissions from a small and shallow lake. Similarly, zones that are shallow, such as littoral zones, have increased rates of ebullition compared to deeper areas within

the same waterbody (Chanton et al., 1989). Atmospheric pressure also has a role in ebullition. In regions of higher altitudes and when barometric pressure drops, ebullition increases (Casper et al., 2000; Smith & Lewis, 1992).

Alternate electron acceptors such as nitrate (NO_3^-), manganese (IV) (Mn^{4+}), iron (III) (Fe^{3+}), and sulfate (SO_4^{2-}) limit methanogenesis. The energy gained by reducing these electron acceptors is greater than the energy gained by reducing CO_2, or acetate, to CH_4. Therefore the microorganisms that undergo more energetically favorable reductions outcompete methanogens (Boon & Mitchell, 1995; Feng, Guo, Chen, Wang, & Du, 2013). Thus, methanogenesis is often limited to environments that have low concentrations of alternate electron acceptors.

Increasing NO_3^- in a stormwater pond can also have the opposite effect as alternate electron acceptors on methanogenesis due to increases in primary productivity (DelSontro, Beaulieu, & Downing, 2018; West, Creamer, & Jones, 2016). Eutrophication, or the increase in the productivity of an aquatic ecosystem, is often a result of increasing nutrient inputs of nitrogen or phosphorus (Carpenter, 2005). Increased nutrient inputs lead to increased algal growth, providing autochthonous labile organic matter (OM) that can fuel methanogenesis (Mengel & Kirkby, 2001). Autochthonous OM influence CH_4 emissions in aquatic ecosystems and so can allochthonous inputs, or the OM that comes from terrestrial material from outside the aquatic ecosystem. If there are high concentrations of OM in the environment, methanogens are able to access the substrates needed to produce CH_4, even when alternate electron acceptors are present. This dynamic is common in freshwater systems where OM is often abundant (Bastviken, 2009). Therefore, an increase in OM typically correlates with an increase in CH_4 production (Boon & Mitchell, 1995). Multiple studies have shown increases in CH_4 ebullition correlated with nutrient enrichment and eutrophication in freshwater ecosystems. (Beaulieu, DelSontro, & Downing,

2019; Davidson et al., 2018; Peacock, Audet, Jordan, Smeds, & Wallin, 2019; Sepulveda-Jauregui et al., 2018). Additionally, eutrophication magnifies temperature sensitivity, meaning that when a freshwater body is higher in trophic level, methanogenesis will change more drastically with changing temperatures (Sepulveda-Jauregui et al., 2018). Based on the responses of other shallow aquatic ecosystems, it is likely that eutrophication in stormwater ponds will result in a net increase in ebullitive CH_4 flux.

Organic matter, alternate electron acceptors, and nutrients highlight the importance of surrounding land use, land cover and regulations within freshwaters. For example, organic matter quantity and quality are linked to watershed size and catchment land use, runoff associated with agricultural land cover tend to have higher levels of NO_3^- compared to urban or forested areas, and in Mexico City minimal regulations on wastewater result in high nutrient levels, leading to exacerbated CH_4 emissions from urban aquatic ecosystems (Martinez-Cruz et al., 2017; Mitrovic & Baldwin, 2016; Vaughan et al., 2017; Williams et al., 2016). Therefore, understanding surrounding land cover and regulations are important in understanding certain drivers of methane emissions.

Eutrophication often creates hypoxic conditions that lead to degradation of aquatic ecosystems (Bricker et al., 2008). Aeration in freshwaters have been used as a common tool since the early 20th century to help limit hypoxia associated with eutrophication by circulating water throughout the system and into the oxygenated atmosphere (Foster, 1994; Schueler, 1987). Since aerators are designed to increase oxygen in the water column, ponds with aerators may have decreased CH_4 emissions due to increased CH_4 oxidation.

Freshwater salinization is an increasing problem in the northeast, particularly in urban areas where impervious surface cover is high (Kaushal et al., 2005). Rising salinity has an impact

on CH_4 emissions from aquatic ecosystems, with laboratory studies showing a 25% reduction in CH_4 flux when salinity changed from 0.8 ± 0.1 $dS.m^{-1}$ to 3-6 $dS.m^{-1}$ (Denier van der Gon and Neue, 1995). This finding is particularly relevant to stormwater ponds, since salt is a common additive to roads and parking lots and these water bodies are often designed to capture run-off from impervious surfaces, resulting in extreme salinization of stormwater ponds due to the use of road salt by municipalities (Marsalek, 2003). Therefore, salinity could be an important driver of CH_4 emissions from stormwater ponds included in this study.

2.0 Objectives and Hypotheses

The main objective of this study was to quantify total CH_4 flux in stormwater ponds and identify which variables were the best predictors of emissions. I hypothesized that stormwater ponds with the highest temperature, shallowest water, highest OM content, highest nutrient concentrations and highest Chl *a* would result in highest CH_4 flux. I also hypothesized that stormwater ponds with highest nitrate concentrations and highest conductivity would result in lowest CH_4 flux. Another objective of this study was to identify seasonal and weather related patterns of CH_4 ebullitive flux in stormwater ponds. I hypothesize that CH_4 ebullition will peak in the summer due to high temperatures, and that ebullition will peak during times of low pressure due to changes in pressure within the sediment, To test these hypotheses, ebullition was measured along with water temperature, conductivity, water depth, %OM, Chl *a,* and sediment and water nutrients from 8 stormwater ponds.

3.0 Materials and Methods

3.1 Site descriptions

Eight stormwater ponds in the Town of Henrietta, NY were studied from June 2019 through October 2020, with 5 stormwater ponds in 2019 and 6 in 2020 (Table 1). Henrietta is in Western New York and is 156 m above sea level. The region has a humid but continental temperate climate that is impacted by the close proximity of the Great Lakes (US Department of Commerce, n.d.). The average temperature is 9.3° C and the average rainfall is 1138 mm (Climate-Data, 2021).

D Lot: This stormwater pond is located on the campus of Rochester Institute of Technology (RIT) and was only sampled in 2020. The D Lot pond was built in 2004 to manage stormwater associated with the construction of the Gordon Field House. It is 1050 m^2 and is 1.6 m at its deepest where water depth ranged 0.13 m. It is lined with large rocks in effort to reduce erosion from the banks and is aerated with a fountain. It is surrounded by manicured lawn and has very little emergent vegetation, with only a very few cattail (*Typha* spp.) and rush (*Juncus* spp.) plants growing by the inlet. There was no visible submerged vegetation.

Egret: This stormwater pond is located in southern Henrietta in the residential neighborhood of Shadow Ridge and was sampled in both 2019 and 2020. The Egret pond was built in 2003 to collect stormwater runoff from the developing neighborhood of Shadow Ridge. It is 1660 m^2 with a maximum depth of 2.1 m, however, pond depth varied 0.89 m throughout the field season. The surrounding landscape is maintained lawn with sparse vegetation including green ash (*Fraxinus pennsylvanica*), cottonwood (*Populus deltoides*), silky willow (*Salix sericea*), silky dogwood (*Cornus amomum*), red maple (*Acer rubrum*), crab apple (*Malus* sp.) and autumn olive (*Elaeagnus umbellata*). The perimeter of the stormwater pond has emergent

cattail (*Typha* spp.) and in the summer there is dense floating vegetation throughout the pond (duckweed, *Lemnoideae* sp.) and visible algal growth.

J Lot: This stormwater pond is located on the RIT campus and was sampled in 2019 and 2020. The J Lot pond was built in 2005 to collect stormwater from adjacent parking lots. It is 3120 m^2, has three forebays and is 2.0 m at its deepest where water depth ranged 0.30 m. The immediate area around the pond is maintained lawn with some cover of cattail (*Typha* sp.) and river birch (*Betula nigra*). Arrowhead (*Syngonium podophyllum*), rush (*Juncaceae* sp.) and purple loosestrife (*Lythrum salicaria*) are also present along the shoreline and there was considerable cover of submerged vegetation including pondweed (*Potamogeton* sp.) and bladderwort (*Utricularia* sp.) throughout the pond. To the west of the pond is forested land, however the majority of surrounding land-use is parking lots.

Martin: This stormwater pond is located in southern Henrietta at the Martin Road Park and was only sampled in 2020. The Martin pond was built around 2002 to collect stormwater following the construction of the park. It is 4370 m^2, 3.7 m at its deepest and water depth ranged 0.17 m. It has both a fountain and bubblers and is lined with clay, a common liner used to limit pond water from seeping into the soil. According the New York State Department of Conservation, stormwater pond liners are necessary when there are extremely permeable soils present such as hydrologic soil group A (Nysdec, 2010). The pond was treated by Clearly Aquatics Inc. with organic blue dye and Cutrine (a copper ethanolamine algicide and herbicide) in May and August 2020. The area around the pond is maintained lawn with sparse vegetation, including planted cottonwood (*P. deltoides)*. No evident emergent vegetation was present in the pond.

Nightfrost: This stormwater pond is located in southern Henrietta in the residential neighborhood of Wintergarden and was only sampled in 2019. The Nightfrost pond was built in 2001 to collect stormwater runoff from the developing residential neighborhood of Wintergarden. It is 1.6 m at its deepest and 6470 m^2. Approximately half of the land adjacent to Nightfrost is forested and the other half is residential. Around 2010, forest was cleared directly adjacent to the pond resulting in 6880 m^2 of wetlands feeding into the undeveloped side of the pond. Vegetation in this wetland area is dominated by cattail (*Typha* spp.) and common reed (*Phragmites australis)*.

Redbridge: This stormwater pond is located in southern Henrietta and is adjacent to the Lehigh Valley Trail, in the residential neighborhood of Sutter's Crossing. Redbridge was sampled in both 2019 and 2020. The Redbridge pond was built in 2003 to collect stormwater from the residential development of Sutter's Crossing. It is 1130 m^2, 0.8 m at its deepest and water depth ranged 0.33 m. Approximately half of the shoreline is forested land and the other half is residential lawn. The surrounding vegetation from the forested side was diverse and included silky dogwood (*Cornus amomum*), silky willow (*Salix sericea*), yellow poplar (*Liriodendron tulipifera*), sumac (*Rhus typhina*), basswood (*Tilia americana*), red oak (*Quercus rubra*), green ash (*Fraxinus pennsylvanica*), honey suckle (Lonicera), buckthorn (*Rhamnus*), common reed (*P. australis*) and golden rod (*Solidago* sp.). The pond was dominated by the macroalgae, stonewort (*Chara* sp.), except by the inlet where storm events washed away submergent plants. In the autumn of both years the pond was covered in a dense layer of algae.

S Lot: This stormwater pond is located on the southeast side of RIT's campus and was only sampled in 2020. The S Lot pond was built in 1998 to collect stormwater from the University Commons dormitories and adjacent parking lots. It is 1130 m^2, 0.8 m at its deepest

and water depth varied 0.13 m. It was previously an aerated pond but was no longer in 2020. It is surrounded by manicured lawn, with sparse cover of planted trees (river birch (*Betula nigra*), swamp oak (*Quercus bicolor*), green ash (*Fraxinus pennsylvanica*) and crab apple (*Malus* sp.)). There was no noticeable submerged vegetation during the measurement period.

Tinker: This stormwater pond is located in eastern Henrietta at the Tinker Nature Park and was only sampled in 2019. The Tinker pond was built around 1996 to receive stormwater runoff from a newly constructed park, where its inflows were connected to parking lots, open fields, pavilions, and playgrounds and its outflow is connected to a natural wetland. In 2016, benthic barriers were installed in order to control the invasive species, *Hydrilla verticillata*. Benthic barriers have been found to be effective at controlling thick infestations of aquatic vegetation (Bailey & Calhoun, 2008). The pond is 2.2 m at its deepest and is 4050 m^2. The surrounding land cover is a mix of emergent wetland dominated by cattail (*Typha* spp.) and common reed (*P. australis*) and forested wetland dominated by beech (*Fagus grandifolia*) and maple (*Acer* spp.).

3.2 Depth

The depth of each stormwater pond was measured using a marked rope with an attached weight. In 2019, depth measurements were taken along transects and each measurement was taken at approximately 2 meters distance from each other. In 2020, depth measurements were only at the bubble trap locations. In 2020, seasonal changes in water height were tracked using a permanent marker that was installed on the side of each pond. A meter stick was then used to measure the change in water depth every time bubble traps were sampled.

3.3 Ebullitive flux

Inverted funnels (bubble traps) were used to measure ebullitive CH_4 flux. A 10 inch funnel was attached via 3:1 heat-shrink tubing to a 60 mL syringe fitted with a one-way stopcock (Wik, Crill, Varner, & Bastviken, 2013). Styrofoam was fit around the funnel to provide floatation. Bubble traps were anchored with a rock tied to polypropylene rope long enough that they could float with an approximate 1.5 meter radius.

The number of bubble traps per pond was determined based on studies that showed that a minimum of 4 bubble traps per 1 acre provided good site coverage (Casper et al., 2000; Wik et al., 2013). Stormwater ponds in this study were approximately 1 acre in size and in 2019, 8-10 bubble traps were deployed in each pond. After examining data from 2019, the level of within pond variability was low therefore bubble trap replicates were reduced to 6 per pond. Bubble traps were placed along two transects to capture variability (Peixoto, Machado-Silva, Marotta, Enrich-Prast, & Bastviken, 2015); 4 traps per transect in 2019 and 3 per transect in 2020. The only exception was J Lot, which had multiple forebays, which 2 forebays were sampled with an extra trap in 2019 (n=10 traps) and then in 2020 one of the forebays was sampled without increasing replicate number (n=6). In 2019, bubble traps were placed in transects according to even increments of depth to capture ebullition from the shallowest and deepest areas in stormwater ponds. However, there was not a noticeable bubble trap location dependence in 2019, so in 2020 bubble traps were placed in approximately even increments of length between traps, where one end of the transect was near shore and the other was around the center of the pond. In 2020, one transect was located near an inflow and, the other, an outflow. This was implemented in effort to capture potential differences in ebullition due to differences in inflow and outflow characteristics.

Bubble traps were accessed using a 2-person inflatable kayak in order to minimize sediment disturbance while sampling (Wik et al., 2013). Traps were sampled approximately every 2 to 3 days, total bubble volume was recorded, then a 10 mL sample was collected and transported back to the lab for analysis. Gas collections were taken, from June 12th to October 30st in 2019. In 2020, COVID-19 lab shutdowns delayed the start of the field season and bubble traps were not deployed until July 17th and sampling then continued until October 26th.

3.4 Diffusive flux

Floating chambers with shields were used to measure diffusive CH_4 flux. Chambers were constructed from a 5 quart bucket with an airtight fitting connected a one-way stopcock inserted in the center for gas sampling. Pool noodles were used to provide flotation and a subsurface shield made of clear vinyl fabric attached to wire mesh was hung 10 cm below the chamber using steel wire to block ebullitive flux (Wik, Thornton, Bastviken, Uhlbäck, & Crill, 2016).

Methane diffusive flux has been showed to have much lower spatial variation than ebullition therefore only 4 chambers were deployed per pond (Wik et al., 2016). Chambers were placed at the beginning and end of each bubble trap transect and rope was used secure them such that they were situated 2 meters from the edge of the transect. Diffusive flux has also been shown to have much lower temporal variability than ebullition. Therefore, floating chambers were only deployed three times in mid-August, mid-September and late October in 2019, and 2 times in 2020 in mid-August and mid-September. However, in 2019 only data from the autumn sampling collection was used due to contamination of gas samples in the first two diffusive deployments. Chambers were deployed for a 24 hour period; the air directly next to the floating chamber was sampled upon deployment to capture t = 0 then air from within the chamber was collected 24

hours later (Bastviken et al., 2010). Samples were collected using 20 mL syringes and were transported back to the lab for analysis.

3.5 Gas analyses

For gas samples collected from bubble traps, a 60x dilution was performed within 24 hours of collection using nitrogen gas as the dilution medium. The diluted sample was injected into pre-evacuated 10mL glass vials with a rubber stopper and aluminum crimp seal. For gas samples collected from the floating chambers, samples were transferred directly into pre-evacuated vials, dilutions were not necessary since CH_4 concentrations were much lower. A Shimadzu gas chromatograph (GC-2014) equipped with an AOC-6000 and a flame ionizing detector was used to determine CH_4 concentration for both diffusive and ebullitive flux.

Additionally, once in summer and fall of 2019, a 10 to 20 mL sample from a subset of bubble traps was injected into pre-evacuated 30 mL glass vials. Enough nitrogen gas was added to each of the 30 mL glass vials to result in 60 mL of total gas. These samples were taken to the University of New Hampshire for $\delta^{13}C\text{-}CH_4$ analysis using an Aerodyne quantum cascade laser (QCL).

3.6 Water chemistry

Dissolved O_2 (DO), conductivity and temperature were measured using a handheld Hach HQ40D meter adjacent to each bubble trap whenever ebullitive gas samples were collected. Measurements were taken at the bottom of the water column in order to represent conditions closer to the sediment.

Water was collected three times in both 2019 and 2020 from each stormwater pond using Whirl-Pak® bags. In 2019, samples were collected on July 31st, August 28th, and on October 29th. In 2020, samples were collected on July 29th, September 3rd and November 4th. Samples were taken from 5 locations in each stormwater pond in 2019: at the beginning and end of the bubble trap transects and in between the transects themselves. In 2020, samples were taken at every bubble trap, resulting in 6 samples per stormwater pond. The water samples were placed in a cooler immediately and filtered through swinnex 24mm Whatman GF/C filters when brought back to the lab. Filtered samples were then stored at -20 °C until they were thawed for analysis. Water samples were analyzed for nitrate, ammonium, and phosphate.

Nitrate concentrations were quantified using vanadium trichloride (VCl_3) and sulfanilamide as the color reagent (Doane & Horwáth, 2003). Ammonium concentrations were quantified using a phenol-hypochlorite method and nitroprusside as the catalyst (Solorzano, 1969). Total inorganic nitrogen concentrations were determined by adding nitrate and ammonium concentrations. Phosphate concentrations were quantified using the ammonium-molybdate method (Murphy & Riley, 1962). All samples were analyzed using a Shimadzu 1800 Spectrophotometer.

In September 2020, four water samples per stormwater pond were collected using 1 liter amber bottles to measure chlorophyll a (Chl *a*). Samples were immediately placed in a cooler, transported to the lab and filtered through GF/F filters until the filters became close to saturated. The volume of water used was recorded and the filter was placed into an aluminum foil pouch and stored at -80 °C for future analysis. For the analysis, 90% acetone was applied to each filter paper and then the filter was ground to extract the Chl *a* from cells (Nielsen, 1998). The ground sample was stored in a freezer overnight and the next day a Shimadzu 1800 Spectrophotometer

was used to determine Chl *a* concentrations through measuring absorbances at 665 and 750 nm before and after two drops of 5% HCl were added to a cuvette.

3.7 Sediment cores

Sediment cores were collected on September 18th, 2019 and August 27th, 2020. In 2019, 5 sediment cores were collected from Egret, J Lot and Redbridge. Tinker was not sampled due to the presence of a benthic barrier and Nightfrost was not sampled due to site access challenges. In 2020, five sediment cores were collected from Egret, J Lot, Martin, Redbridge and S Lot. D Lot was not sampled because it was lined with large rocks. Cores were placed into a cooler and transported to the lab and immediately separated into 4 sections of 5cm. Cores from Martin did not have sediment below 10cm and cores from S Lot did not have sediment below 15cm. In 2019, the sediment was passed through a #8 sieve (2.38 mm opening) and in 2020 no sieve was used. Sediment cores were used to determine CH_4 production and oxidation potential, extractable nitrate and ammonium, total phosphorus and OM.

3.8 Incubation experiments

Potential rates of CH_4 production and oxidation were measured on sediment core depths of 0-5 cm and 10-15 cm. For both production and oxidation experiments, 50 and 100 grams of sediment were weighed, respectively, and placed into airtight mason jars fitted with thick rubber stoppers. Twenty-five grams of sediment for each sediment core were placed in a 60 °C oven for a week and weighed before and after drying to determine total dry sediment in each mason jar. For both production and oxidation experiments, the height of the sediment in each jar was measured. Water was added to empty mason jars and then measured in a graduated cylinder to

determine volume of the headspace for each sediment height. For the production experiment, anaerobic conditions were established for potential CH_4 production incubations by adding 50 mL of sparged water and flushing with N_2. Mason jars were incubated in the dark at 22 °C for 2 to 4 weeks. The jars were then flushed with N_2 and the first set of gases were sampled the following day (Duc, Crill, & Bastviken, 2010; Hodgkins et al., 2014). Gas samples were collected a total of eight times, such that t = 0 through t = 3 were taken every 24 hours and t = 4 to t = 7 were taken every 2 to 3 days. At each sampling time point, 11 mL of N_2 was injected into the mason jar, sample was plunged up and down three times, and 11 mL of sample was taken and injected into an evacuated vial. For CH_4 oxidation potential, jars were spiked with 11 mL of 40% CH_4 to reach a headspace CH_4 concentration of 1% and sampling began immediately after spiking (Duc et al., 2010; Larmola et al., 2010). Gas samples were collected a total of seven times, such that t = 1 was taken 4 hours after spiking, t = 2 was taken 12 hours after spiking and t = 3 was taken 24 hours after spiking. From t = 3 to t = 6, samples were collected every 24 hours. For each sampling point for oxidation, 11 mL of air was injected into the mason jar, gas was plunged up and down three times, and 11 mL of sample was taken and injected into an evacuated vial. Gas samples were analyzed on a GC as described previously and rates of CH_4 production and oxidation were calculated by CH_4 concentration, headspace volume, and the dry weight of the sediment.

3.9 Sediment chemistry

Sediment nitrate and ammonium were extracted using KCl (Maynard, Kalra, & Crumbaugh, 1993). Five mg of sediment was placed into a centrifuge tube and another 5 mg was placed in a 60 °C oven for 24 hours to determine dry sediment weight. Fifty mL of 2M KCl was

added to each centrifuge tube. Centrifuge tubes were placed horizontally on a shaker for 30 minutes and then centrifuged for 10 minutes at 5000 rpm. The supernatant was filtered using swinnex 24mm Whatman GF/C filters and placed in the -20°C freezer until analysis. In 2019, only sediment depths of 5-10cm and 15-20cm were analyzed for nitrate and ammonium. In 2020, all sediment depths were analyzed for nitrate and ammonium. For total phosphorus, 0.5mL of 50% magnesium nitrate was added to 100 mg of dry and ground sediments. These samples were ashed at 550°C for 2 hours and, once cool, 10mL of 1M sulfuric acid was added, vortexed, and shaken for 16 hours. Once the sediment settled in the solution, the supernatant was diluted 10x. Analysis of nitrate, ammonium and phosphorus followed the same procedure noted for water nutrients in section 4.8; however, the extraction media was used as the solvent for the standards instead of nanopure water.

OM was determined using the loss on ignition method (Heiri, Lotter, & Lemcke, 2001). Approximately 20mg of sediment was placed into a 60 °C oven to obtain the dry weight of the sample. Dried samples were put into a muffle furnace at 550 °C for 4 hours and reweighed.

3.10 Weather data

Air temperature, atmospheric pressure and precipitation data came from the Greater Rochester International Airport Station and was accessed online through Weather Underground ("Rochester, NY Weather History | Weather Underground," n.d.). Data were selected every hour from the beginning to the end of bubble trap deployment. For the determination of average temperature, pressure, precipitation and pressure that correlated with each ebullitive flux measurement, data were averaged from the time bubble traps were reset to the time they were

sampled. Maximum and minimum pressure were also determined for each time frame correlating to ebullitive flux.

3.11 Statistical analyses

All statistics were performed using RStudio Version 1.4.1106. Each dataset was evaluated for homogeneity of variance and normality prior to statistical analysis. A Kolmogorov-Smirnov test showed that the CH_4 ebullition dataset was not normally distributed, therefore nonparametric tests were used for this dataset. All other datasets met the assumptions of parametric tests.

Kruskal-Wallis tests were used to analyze ebullition differences amongst sites from years separated and combined. When significant differences were found, Fisher's LSD post hoc tests were used. Summer and autumn were separated where summer was classified as June 21st to September 21st and Autumn was classified as September 22nd to October 30th. Kruskal-Wallis tests were also used to determine ebullition differences between months. Nightfrost was omitted from autumn and monthly statistics since there was no October data for Nightfrost.

Kendall rank correlation tests were used with a Bonferroni correction to analyze correlations between CH_4 ebullition and water temperature, DO, conductivity, water depth, change in water depth, air temperature and average, minimum and maximum atmospheric pressure. This analysis produced a Tau (τ) correlation coefficient output from -1 to 1, where values closest to 0 had the weakest correlations. τ values greater than or equal to |0.5| were considered to have a strong correlation, between |0.3| and |0.5| were considered moderate correlations, between |0.1| and |0.3| were weak correlations, and any τ value below |0.1| were considered very weak (Cohen, 2013). Only correlations with $p < 0.05$ were interpreted. The

Bonferroni correction was used to minimize the error associated with numerous ponds being evaluated within the same correlation test (Armstrong, 2014).

One-way ANOVAs were used to identify differences in diffusive flux, potential CH_4 production rates, potential CH_4 oxidation rates, chlorophyll-a, OM content, sediment nutrients and $\delta^{13}C$-CH_4 amongst ponds. For diffusive flux, years were not separated in determining differences amongst ponds. For all sediment nutrients, OM, potential CH_4 production and oxidation, both the year and sediment depth were analyzed separately when determining differences amongst ponds. Differences between season and isotopic composition were identified through a one-way ANOVA. For measurements that had a seasonal component (water nutrients, water temperature, DO, conductivity), a full-factorial two-way ANOVA with pond and month or sampling date as fixed factors was used. For water nutrient two-way ANOVAs, 2019 and 2020 data were separated. For water temperature, DO and conductivity, results shown are from separated years and years combined. For all two-way ANOVA analyses, Nightfrost was not included in the statistics since it is missing data from autumn. When significant effects were identified, a Tukey HSD post-hoc test was used to determine the differences amongst means.

An independent t-test was used to examine differences in spatial variability of DO within aerated and non-aerated ponds. Spatial variability of DO was calculated by finding the daily range of DO per pond.

Linear regressions were used to analyze the trends between average ebullition and diffusion, production, oxidation, temperature, DO, conductivity, Chl *a*, ^{13}C, depth, OM 0-5cm, sediment nutrients and water nutrients. The regressions were performed on 2019, 2020, and both years from the beginning to the end of the field season. Because data from linear regressions

were based on ebullition and corresponding data from the entire field season, Nightfrost was omitted as a data point since there was no autumn data.

4.0 Results

4.1 Water and sediment characteristics

Across all ponds and dates water temperature averaged 21.5 ± 0.1°C, and there was significant seasonal variation ($p < .0001$; Table 2a) and differences amongst ponds ($p < .0001$; Table 2a). Water temperature dropped 44% from July (25.2 ± 0.1°C) to October (14.0 ± 0.1°C), and S Lot had the highest temperature (23.8 ± 0.4°C) and D Lot had the lowest (19.8 ± 0.4°C, Table 2b, Figure 2).

Across all ponds, DO varied significantly by season ($p < .0001$, Table 2a), increasing by 4.5 mg/L from June (6.4 ± 0.6 mg/L) to September (10.9 ± 0.2 mg/L; Table 2b, Figure 2). DO was also significantly different amongst ponds ($p < .0001$, Table 2a), where the highest DO concentrations, found in S Lot (14.9 ± 0.3 mg/L), were 3x higher than the lowest, found in Egret (5.3 ± 0.23 mg/L; Table 2b). DO concentrations during the warmer months reached very low levels nearing 0 mg/L, particularly at Egret (Figure 2). Average DO in ponds with aeration (8.80 ± 0.147 mg/L) was not higher than ponds without aeration (10.5 ± 0.262 mg/L). However, the average daily range of DO within aerated ponds of 1.75 ± 0.160 mg/L was significantly lower than non-aerated ponds of 6.61 ± 0.436 mg/L ($p < .0001$). This signifies that DO in aerated ponds had significantly less spatial variability within ponds

Conductivity averaged 767 ± 7 µS/cm and significantly varied by season ($p < .0001$; Table 2a) and pond ($p < .0001$; Table 2a). Conductivity decreased 40% from June (930 ± 82 µS/cm) to October (569 ± 10 µS/cm) and the pond with the highest average conductivity, S Lot (1170 ± 29 µS/cm), was ~3x higher than the pond with the lowest, Martin (438 ± 3 µS/cm; Table 2b, Figure 2).

The average Chl *a* concentration across all ponds was 29.1 ± 5.0 µg/L with significant variation amongst sites ($F_{5,24} = 3.39$, $p = .03$). Ponds with the highest Chl *a* were D Lot (46.7 ± 2.3 µg/L), Egret (41.2 ± 10.9 µg/L) and Redbridge (46.2 ± 19.2 µg/L) and they were approximately 13x higher than the pond with the lowest Chl *a*, Martin (3.5 ± 0.9 µg/L; Figure 3).

Across all ponds, water column NO_3^-, TIN and PO_4^{3-} concentrations averaged 75.0 ± 14.0 µgN/L, 177 ± 21.0 µgN/L and 27.0 ± 2.00 µgP/L, respectively. Redbridge had the highest water column concentrations of NO_3^- and TIN for both 2019 ($p < .001$) and 2020 ($p < .0001$), whereas Egret had the highest water PO_4^- in 2020 (2020: $p < .0001$; Table 3b). There were also statistically significant differences between all water nutrients and collection date, although not all differences were significant in both years (Table 3a). For nitrogen species, concentrations were higher in autumn (NO_3 2020: $p < .0001$, TIN 2019 & 2020: $p < .0001$), whereas PO_4^{3-} was statistically highest in summer (2020: $p < .0001$; Table 3a and 3c, Figure 4). Water TIN^- concentrations were generally higher in 2020 than they were in 2019, where the biggest difference was at Redbridge by 4x (Table 3b and Table 3c).

Sediment NO_3^-, TIN and TP concentrations for the 0 to 5 cm depth profile across all ponds averaged 7.09e-05 ± 4.74e-05 mgN/g dry sediment, 0.052 ± 0.009 mgN/g dry sediment and 0.904 ± 0.073 mgP/g dry sediment, respectively. All nutrients in the water and sediment, except sediment NO_3^- ($F_{4,15} = 2.1$, $p = .13$), varied significantly amongst sites (Table 3a and 3b). Sediment NO_3^- did not vary amongst ponds due to extremely low concentrations. There was about a 3000x higher concentration of NH_4^+ in the sediment than NO_3^-, leading to significant differences in TIN amongst sites (0-5 cm: $F_{4,15} = 3.1$, $p = .05$; 2020 5-10 cm: $F_{4,15} = 7.5$, $p = .002$). Egret, J Lot and Redbridge had similar TIN concentrations in the sediment while S Lot

and Martin had relatively low TIN. There were also significant differences in TP amongst ponds (0-5: $F_{4,15} = 20$, $p < .0001$), where Egret TP was about 3x higher than S Lot TP (Figure 5).

Sediment %OM varied with site (0-5cm: $F_{4,15} = 10$, $p < .001$) with values ranging from 2.88 ± 0.754% to 12.1 ± 0.857%. At the 0-5cm depth, J Lot, Egret and Redbridge had similarly highest %OM. However, at the 5-10 depth, Redbridge remained high in OM and was statistically different from J Lot and Egret (2020: $F_{4,15} = 21.2$, $p < .0001$). At 0-5cm, Martin and S Lot had the lowest % OM, with values of 3.42 ± 0.670 and 2.88 ± 0.754%, respectively (Figure 6).

4.2 Temporal variation of CH_4 flux

From June to October, overall ebullition was 257 (median: 173) mg CH_4 m^{-2} d^{-1}, where there was substantial seasonal variation. The overall average summer ebullition from June 21st to September 21st for all eight ponds studied was 312 (median: 239; Table 4) mg CH_4 m^{-2} d^{-1}, whereas the overall average autumn ebullition from September 22nd to October 30th was 77.1 (median: 17.5; Table 5) mg CH_4 m^{-2} d^{-1}. Average CH_4 ebullition was 4x greater (median: 14x greater) in summer than autumn. Across years, July had the greatest CH_4 ebullition (average: 386; median: 326 mg CH_4 m^{-2} d^{-1}) and October had lowest (avg: 50.9; median: 9.79 mg CH_4 m^{-2} d^{-1}; Table 6).

Kendall rank correlations provided insight into drivers of seasonal patterns of CH_4 ebullition. There were significant correlations ($p < .0001$) between ebullition and both air temperature and water temperature. For air temperature $\tau = .32$ and for water temperature $\tau = .24$. Both of these Kendall Tau values show positive relationships between temperature and ebullition; air temperature had a moderate correlation and water temperature had a weak correlation. Kendall rank correlations also illustrated that DO ($\tau = -.0627$, $p < .0001$), water

depth (τ = -.259, p < .0001) and precipitation (τ = -.102, p < .0001) negatively correlated to ebullition and conductivity positively correlated with ebullition (τ = .183, p < .0001, Table 7).

The $\delta^{13}C$ composition of CH_4 ebullition also showed significant seasonality ($F_{1,41}$ = 11.2, p = .002). Averaged across ponds, fluxes were lighter in summer (-63.4 ± 1.0 ‰, avg ± SE, Figure 22) than in autumn (-51.2 ± 4.1 ‰, avg ± SE, Figure 7).

Ebullition was episodic in all ponds, with periodic jumps in flux occurring throughout the measurement period (Figure 8). Ebullition was most episodic in nature in the ponds with the highest overall ebullition fluxes, particularly Nightfrost and Redbridge. Some peaks in ebullition aligned with decreases in atmospheric pressure, partially explained by the significant positive correlation between low atmospheric pressure and ebullition (p = .004, τ = .044). This correlation was significant, but extremely weak. Maximum atmospheric pressure correlated more strongly (although still a weak correlation) to ebullition (p < .0001, τ = -.233) than minimum atmospheric pressure. In addition to seasonal patterns associated with air temperature, spikes in air temperature were also associated with peaks in ebullition (Figure 8). When examining the linkage between episodic variation ebullition and temperature, a Kendall correlation test was run on only summer values to omit temperature's seasonal effect. This correlation between summer ebullition and air temperature was significant and positive (p < .0001; τ = .18).

CH_4 diffusive flux averaged 10.6 ± 1.41 mg CH_4 m^{-2} d^{-1} across sites and dates, only 4% of total CH_4 flux. Diffusive flux measurements were taken much less frequently than ebullitive flux measurements, therefore, it was harder to identify temporal trends. However, from the diffusive data that was collected, there was no evidence that diffusion varied significantly over time ($F_{2,56}$ = 0.961, p = .4, Figure 9).

4.3 Variation across ponds of CH_4 flux

Pond ebullition varied significantly amongst ponds ($p < .0001$; Table 3 and 5). Redbridge had the highest overall ebullition, where average and median ebullition was 476 and 350 mg CH_4 m^{-2} d^{-1}, respectively. The variation in ebullition amongst sites was so large that ebullition from Martin (avg: 17.5; median: 0.296 mg CH_4 m^{-2} d^{-1}; Table 3) was 27x and 1200x less than Redbridge's average and median ebullition, respectively. Martin's ebullition rates were so low that they were 18x lower than the average ebullition in Tinker, the pond with the second lowest ebullitive flux. Across years, summertime rates of ebullition were highest in Nightfrost and Redbridge, Egret and S Lot had medium-high rates of ebullition, D Lot had medium-low rates of ebullition, J Lot and Tinker had low rates of ebullition and Martin had extremely low ebullition (Figure 10, Table 4).

The summertime $\delta\,^{13}C$-CH_4 signature of ebullition varied significantly across ponds ($F_{4,28} = 3.54$, $p = .02$) with values ranging from -67.4 ± 1.5 ‰ at Redbridge to -59.8 ± 1.7 ‰ at J Lot. In Autumn, values did not differ significantly ($F_{3,14} = 1.21$ $p = .4$) and ranged from -37.3 ± 14 ‰ at Egret to -57.6 ± 8.53 ‰ at Redbridge (Figure 7).

Diffusive flux was more consistent across ponds than ebullition; however, there were significant differences amongst ponds ($F_{7,52} = 3.79$, $p = .003$). Egret had the highest diffusive flux (17.8 ± 5.7 mg CH_4 m^{-2} d^{-1}) while J Lot, Martin and D Lot had the lowest (J Lot: 5.0 ± 0.8; Martin: 2.7 ± 0.4; D Lot: 4.3 ± 0.6 mg CH_4 m^{-2} d^{-1}; Figure 9). Overall, patterns in diffusive flux amongst ponds generally tracked those observed for ebullition. Linear regression analyses for 2020 ($R^2 = .58$, $p = .05$) and both years combined ($R^2 = .54$, $p = .04$) indicate that diffusive flux and ebullitive flux trended together (Table 8).

Depth was found to be an important driver to ebullition in our study (R^2 = .84, p = .002). Water TIN in 2019 (R^2 = .99, p = .001) was also significant in predicting CH_4 emissions. Temperature, DO, conductivity, Chl *a*, OM and all other nutrients were not found to be significant drivers of ebullition (Table 8).

4.4 Potential CH_4 production

Potential CH_4 production rates in sediments from 0-5cm significantly differed across sites ($F_{4,19}$ =7.65, p = .001; Figure 11). Redbridge had the highest potential production rates (62.7 ± 19.1 $mgCH_4$ $d^{-1}g$ dry $sediment^{-1}$), Egret had a medium-high production rate (52.6 ± 6.4 $mgCH_4$ $d^{-1}g$ dry $sediment^{-1}$), J Lot had a medium-low rate (21.5 ± 3.8 $mgCH_4$ $d^{-1}g$ dry $sediment^{-1}$), and Martin and S Lot had the lowest rates (Martin: 11.4 ± 4.2; S Lot: 3.2 ± 2.9 $mgCH_4$ $d^{-1}g$ dry $sediment^{-1}$; Figure 11). S Lot had relatively low production at 0-5cm but relatively high ebullition (Figure 10, Table 4 and 5). When ignoring S Lot, production rates tracked ebullition rates ($F_{1,2}$ = 49.0, R^2 = .940, p = .02), where higher production rates were observed in ponds with higher ebullition. Production also trended with %OM (R^2 = .90, p = .01; Table 8). Potential CH_4 production rates across years in sediments from 10-15cm showed no significant differences across ponds (2019: $F_{2,11}$ = 1.45, p = .3; 2020: $F_{3,12}$ =0.458, p = .7). Potential production rates from 10-15cm were much lower, about 22x lower than what was seen in 0 to 5 cm sediments in 2020 and 3x lower in 2019 (Figure 10).

4.5 Potential CH_4 oxidation

Potential CH_4 oxidation rates in 0 to 5 cm sediments followed the same trend amongst ponds as was seen for CH_4 production (R^2 = .86, p = .02, Table 8) where there were significant

differences ($F_{4,20}$ =4.97, p = .01). Redbridge had the highest rates (-59.8 ± 6.37 1 $mgCH_4$ d^{-1}g dry $sediment^{-1}$), Egret and J lot had similarly moderate rates (Egret: -53.6 ± 13.9; J Lot: -42.1 ± 7.2 1 $mgCH_4$ d^{-1}g dry $sediment^{-1}$), and Martin and S Lot had the lowest oxidation potentials (Martin: -16.6 ± 3.6; S Lot: -13.3 ± 2.9 1 $mgCH_4$ d^{-1}g dry $sediment^{-1}$). Similar to trends in production potential, S Lot had relatively low oxidation rates but relatively high ebullition (Figure 10, Table 4 and 5). Differences in potential oxidation across ponds followed the same pattern as ebullition when ignoring S Lot ($F_{1,2}$ = 37.4, R^2 = .924, p = .03), where higher oxidation rates were observed in ponds with higher ebullition. Potential rates of CH_4 oxidation at 10-15 cm were also significantly different amongst ponds ($F_{3,16}$ =5.16, p = 0.02**).**

5.0 Discussion

5.1 Water quality in stormwater ponds

Eutrophication, or high rates of plant and algal productivity, is affecting water bodies globally and can be a substantial driver of low water quality in urban aquatic ecosystems. High nutrient inputs into aquatic ecosystems can result in explosions of algal growth followed by die off, leaving ecosystems hypoxic, decreasing ecosystem biodiversity and sometimes yielding harmful algal blooms (Bricker et al., 2008). Additionally, eutrophication not only increases CH_4 emissions (West et al., 2016), but can also increase the temperature sensitivity of methanogenesis, suggesting that climate warming will exacerbate the impacts of eutrophication on net CH_4 emissions from aquatic ecosystems (Sepulveda-Jauregui et al., 2018). This makes evaluation of the trophic state of stormwater ponds an important consideration for understanding current and future greenhouse gas emissions from these systems.

The trophic state of a waterbody can be assessed both by direct measurements of nutrients and by analyzing Chl *a* concentration. The Carlson's Trophic State Index classifies any waterbody with Chl *a* between 20 and 56 µg/L as eutrophic, identifying the stormwater ponds in this study, which had an average Chl *a* concentration of 29.1 ± 4.99 µg/L, as eutrophic (Carlson, 1977). Phosphorus concentrations can also be used to help determine trophic level, since phosphorus is often the limiting nutrient in freshwater ecosystems (Schindler, 1977). According to Auer, Kieser, and Canale (1986), freshwater ecosystems with PO_4^{3-} concentrations greater than 8.0 µg/L are considered eutrophic and stormwater ponds in this study were well above this threshold, with an average of 27.0 ± 1.7 µg P/L. Both these metrics characterize stormwater ponds in this study as eutrophic, a cause for concern for both the health of the ecosystem and a potential driver of CH_4 emissions from these systems. Nitrogen can also be used to examine

trophic state, however, total nitrogen is used in the index and total inorganic nitrogen is what was measured in our study (Kratzer & Brezonik, 1981). Thus, nitrogen as an indicator of trophic status was not directly assessed. A caveat to using phosphorus or nitrogen as a trophic level indicator in the studied stormwater ponds is that the limiting nutrient in these systems is unknown. Thus, nitrogen may be a better trophic state indicator than phosphorus and vice versa.

Dissolved oxygen is an additional water quality indicator that is linked to eutrophication and impacts a range of ecosystem functions including CH_4 cycling. Methanogens and methanotrophs are anaerobic and aerobic organisms, respectively, making net CH_4 emissions sensitive to DO conditions. The United States Environmental Protection Agency states that DO levels in water bodies below 3 mg/L are of concern and below 1 mg/L are generally devoid of life (EPA, 2016). The average DO from our study of 8.8 ± 0.1 mg/L was above the minimum DO threshold set by the EPA. However, in some ponds, such as J Lot and Egret, DO levels often dropped below 3 mg/L and in the summer DO levels in Egret dropped below 1 mg/L. Low levels of oxygen in the summer are often observed in aquatic ecosystems due to reduced solubility of oxygen at warmer temperatures (MacPherson, Cahoon, & Mallin, 2007). Water column DO concentrations do not necessarily reflect levels of oxygen in the sediment, upper layers of sediment are often anaerobic even when the water column is oxygenated (Grossart, Frindte, Dziallas, Eckert, & Tang, 2011). However, water column DO does affect the magnitude of methane oxidation that can occur in the water column, with periods of low oxygen linked to extremely low levels of methane oxidation (King, 1990). This can translate into increased diffusive CH_4 flux, since less CH_4 diffusing through the water column is consumed by methane oxidizing bacteria before reaching the surface.

Rising salinity, largely the result of road salt inputs in the northeast (Kaushal et al., 2005), is an additional factor that leads to the degradation of aquatic ecosystems resulting in toxic effects on plants, invertebrates and microorganisms, including methanogens (Mitchell & Richards, 1992; van der Gon & Neue, 1995). Conductance measurements such as those used in this study can be used as a metric for salt inputs into aquatic ecosystems, with high conductance associated with high salinity. There are very few government guidelines for thresholds on conductivity (Gensemer, Canton, DeJong, Wolf, & Claytor, 2011), however, Zhao et al. (2016) identified a benchmark level of 249 µS/cm necessary for 95% of macroinvertebrate genera to survive within a river basin ecosystem. The average conductivity amongst ponds in our study, 767 ± 8 µS/cm, is much higher than that benchmark, suggesting that the organisms within the studied ponds were impacted by high conductance. The ponds with the highest conductance levels were located in ponds that collected run-off from parking lots on RIT's campus. This is consistent with findings from Kaushal et al. (2005) that showed salinization as a function of increased impervious surface due to utilization of road salt in winter months.

5.2 Magnitude of CH_4 flux

In this study, total CH_4 flux of 268 mg CH_4 m^{-2} d^{-1} from urban ponds was comparable to CH_4 flux data from urban bodies of water. Herrero Ortega et al. (2019) found that urban freshwaters, including lakes, ponds, rivers and streams had an average of 219 ± 490 mg CH_4 m^{-2} d^{-1}. However, Martinez-Cruz et al. (2017) found that urban bodies of water in Mexico, including reservoirs, lakes, ponds, chinampas, canals and rivers, had an average flux of 8,400 ± 6,900 mg CH_4 m^{-2} d^{-1}. This is much greater than what was found in our study. Interestingly, Martinez-Cruz et al. (2017) found that urban ponds had the lowest CH_4 flux (20 ± 100 mg CH_4 m^{-2} d^{-1}) out of all

the urban aquatic ecosystems studied, and Herrero Ortega et al. (2019) found that urban ponds had the greatest CH_4 flux (503 ± 699 mg CH_4 m^{-2} d^{-1}). However, this mismatch in findings may be a result of ponds from Martinez-Cruz et al. (2017) being inundated only during the hot and wet season in August and September. In comparison to urban waterbodies, natural wetlands from 40-50°N showed an average of 120 mg CH_4 m^{-2} d^{-1} (Cao, Gregson, & Marshall, 1998), temperate lakes from Quebec showed an average of 17.6 mg CH_4 m^{-2} d^{-1} (DelSontro, Boutet, St-Pierre, del Giorgio, & Prairie, 2016), and research from temperate streams in Wisconsin showed an average of 156 mg CH_4 m^{-2} d^{-1} (Crawford et al., 2014).

There is a large range of average CH_4 flux found in urban ponds, the lowest reported flux is 20 ± 100 mg CH_4 m^{-2} d^{-1} (Martinez-Cruz et al. 2017) and the highest flux is 503 ± 699 mg CH_4 m^{-2} d^{-1} (Herrero Ortega et al. 2019). For urban waterbodies that were artificially constructed for stormwater control, the results of this study fall within the higher end of reported emissions. In a study of 15 stormwater ponds in Virginia, Gorsky et al. (2019) measured emissions of 362 mg CH_4 m^{-2} d^{-1}, a flux that is comparable to measurements in this study, especially considering the more southern location. Other artificial pond flux estimates are lower, with values ranging from 30.3 mg CH_4 m^{-2} d^{-1} in Swedish ponds (diffusive flux only; Peacock et al. 2019) to 120 mg CH_4 m^{-2} d^{-1} and 129 mg CH_4 m^{-2} d^{-1} in the Netherlands (van Bergen et al. 2019) and Australia (Grinham et al. 2018), respectively (Table 9).

Large variations in CH_4 flux amongst studies may have had to do with variations in sampling. For example, Ortega et al. (2019) deployed floating chambers very infrequently and only from 8 am to 12pm. Infrequent measurements may capture diffusive flux appropriately but many more measurements are needed in order to accurately determine ebullitive flux (Wik et al., 2016). This is due to the spatiotemporal variability and episodic nature of ebullition.

Additionally, not collecting measurements over a period of 24 hours does not capture diurnal variability, where flux during the day has been seen to be twice as high as flux at night (Bastviken, Cole, Pace, & Tranvik, 2004). Peacock et al. (2019) found emissions to be very low; however, this is likely to do with sampling methods since Peacock et al. (2019) only measured diffusive flux. This does not accurately represent total flux since ebullition is often the dominant pathway in open freshwater systems and in urban ponds (Bastviken et al., 2010; Casper et al., 2000; Martinez-Cruz et al., 2017). Other variations in average CH_4 flux amongst studies could have come from differences in both location and sampling dates, due to differences in temperature. For example, Peacock et al. (2019) only sampled in May and June where temperatures were not likely representative of the entire year. Similarly, our study did not represent the entire ice-free season, where data was not collected in April, May or November Other studies including van Bergen et al. (2019), Herrero Ortega et al. (2019) and Martinez-Cruz et al. (2017) collected data from all seasons.

Ebullition accounted for 96% of CH_4 emissions from ponds in this study. Ortega et al. (2019) and van Bergen et al. (2019) found that ebullition was the most significant pathway for CH_4 flux, where ebullition accounted for 71% and 75% of flux, respectively. Ebullition as the dominant pathway of CH_4 emissions from open water has been well established in literature (Bastviken et al., 2010; Casper et al., 2000; Martinez-Cruz et al., 2017; Natchimuthu et al., 2014). Additionally, the dominant role of ebullition over diffusion in stormwater ponds may be strengthened by the fact that both eutrophication and rising temperature have been shown to increase ebullition but not diffusion (Aben et al., 2017; West et al., 2016). Thus, neglecting to collect ebullition data from open waters, including stormwater ponds, is problematic and will vastly underestimate CH_4 emissions.

Average δ^{13}C-CH4 of -59.1 ± 1.71 ‰ found from our study falls within what has been seen in shallow temperate lakes (Woltemate, Whiticar, & Schoell, 1984) and suggests that acetoclastic methanogenesis is the dominant source of CH_4 (Chanton et al 2005, Whiticar, 1999).These results are also consistent with observations in northern lakes, where ebullition from shallow lake zones have relatively light ^{13}C-CH_4 signatures (Wik et al. 2020).

5.3 Temporal variability of CH_4 flux

Seasonality in methanogenesis due to changes in temperature has been well documented (Aben et al., 2017; Boon & Mitchell, 1995; Duc et al., 2010; Van Hulzen, Segers, Van Bodegom, & Leffelaar, 1999). Bastviken (2009) reported that a decrease in temperature of 10°C would decrease methane production about 4x. Greatly similar to what was reported by Bastviken (2009), a decrease in temperature from July to October of ~11°C aligned with ebullition decreasing 4x from summer to autumn in this study. In contrast to ebullition, CH_4 diffusion in our study was not seen to change seasonally, which is consistent with research showing relatively low temperature sensitivity of CH_4 diffusive flux (Aben et al., 2017).

A limitation to this study is that CH_4 flux was not captured during the spring or winter seasons. Spring and winter often have much lower flux than in the summer (Xing et al., 2005), however, CH_4 data from stormwater ponds are very limited and thus exact seasonal patterns are not certain. Future research to quantify methane emissions from all seasons would be appropriate to determine yearly CH_4 emissions.

The change in average δ^{13}C-CH_4 from summer to autumn of -63.3‰ to -51.2‰ indicates an increase in methanogen production through acetate fermentation over hydrogenotrophy in the autumn (Chanton et al., 2005). This could be due to lower temperatures in autumn favoring

acetate over propionate formation, leaving an abundant supply of acetate for methanogens (Conrad, 2002). The trend seen in our study of an increase in ^{13}C abundance in the colder season is opposite what has typically been observed in the literature (Avery & Martens, 1999; Chanton & Martens, 1988; Jędrysek, 1999), however, isotopic data from lakes and ponds is limited and detailed evaluation of seasonality in Arctic lakes showed no seasonal $\delta^{13}C$ trends.

The episodic nature of ebullition seen in our study is well documented (ie Burke et al., 2019; Wik et al., 2013). Oftentimes, episodic nature can be attributed to lowering atmospheric pressure, as seen throughout literature and through our study (Mattson & Likens, 1990; Scandella et al., 2011). Additionally, temperature changes that were seen to have triggered ebullition have been documented throughout literature (Aben et al., 2017). Ebullition from shallow ponds in particular are increasingly sensitive to temperature changes, since there is less water to regulate temperature, leading to greater episodic ebullition due to atmospheric temperature changes (Burke et al., 2019).

In our study, maximum atmospheric pressure relating to each ebullitive flux measurement correlated more strongly to ebullition than did average atmospheric pressure or minimum atmospheric pressure (Table 7), indicating that high atmospheric pressure had more of an effect on stifling ebullition than low pressure did on encouraging ebullition. Perhaps this can be attributed to rising water depths associated with low atmospheric pressure systems subduing the effects of decreasing atmospheric pressure. Evidence for this suggestion is that precipitation was seen to significantly and negatively correlate to ebullition from our study ($p < .0001$; $\tau = -.102$; Table 7). Since precipitation often comes with low atmospheric pressure, a positive, not negative, correlation to ebullition would be expected. However, precipitation is also known to

increase water depth in ponds (Environmental Protection Agency, 2009), increasing barometric pressure, and potentially decreasing ebullition.

5.4 Differences in CH_4 flux amongst ponds

As expected, depth was found to be an important driver in predicting CH_4 ebullition in our study. Past literature has documented the dependence of ebullition on depth with lower hydrostatic pressure increasing ebullition (Bastviken et al., 2004). Shallow waters also mean there is less opportunity for CH_4 to interact with methanotrophs in the water column, increasing CH_4 emissions (Bastviken, 2008). However, Burke et al. (2019) saw an opposite trend where the shallower ponds were the lowest in CH_4 flux.

The ponds that were highest in water TIN were high in ebullition in our study. Peacock et al. (2019) and van Bergen et al. (2019) also saw a positive relationship between CH_4 emissions and nutrients in stormwater ponds. Nitrogen can be an indicator of trophic status, thus providing evidence that that trophic status relating to nitrogen correlated to increased CH_4 emissions in our study. Sepulveda-Jauregui et al. (2018) found that eutrophic ecosystems are more sensitive to changes in temperature, creating concern since an increase in global urbanization is leading to increasing urban water bodies, often high in nutrients, and global temperatures are increasing as well (Bocquier, 2005; Herrero Ortega et al., 2019; Martinez-Cruz et al., 2017; Sepulveda-Jauregui et al., 2018; Waajen, Faassen, & Lürling, 2014). Nitrate as an alternate electron acceptor did not have a large impact in this study as previously hypothesized. This is likely to do with nitrate levels being incredibly low in sediment, where the microbial activity takes place.

The range in water nutrient concentrations overtime varied substantially (Figure 4). This variation likely had to do with the nature of stormwater, where storm events bring and flush large

volumes of water, drastically changing water chemistry. This variation in nutrient concentrations, likely related to when ponds were sampled relative to storm events, indicates that more consistent measurements of water nutrients would have provided additional insights in this study. Because of the flashy nature of water nutrients in stormwater ponds, sediment nutrients could be the better indicator of nutrient status. Unexpectedly, sediment nutrient patterns did not correlate with ebullition patterns amongst ponds. However, sediment cores were only collected from five of the eight ponds studied limiting the ability to identify a relationship between sediment nutrients and ebullition.

Water TIN^- concentrations in 2019 were generally lower than what was seen in 2020 (Table 3a and Table 3b). This difference in TIN could be due to the flashy nature of water nutrients in stormwater ponds. However, in 2020, one of the six water samples per pond and sampling date was by an inlet, where in 2019 this was not true. Inlets are often higher in nitrogen concentrations than elsewhere in a stormwater pond (Ivanovsky et al., 2018), possibly driving the increased TIN in 2020.

There was no evidence that differences in DO amongst ponds impacted CH_4 ebullition, as identified by linear regressions ($p = .24$, Table 8). Albeit, there was an extremely weak negative correlation that existed between ebullition and DO as identified by Kendall correlation ($\tau = -.06$, $p < .0001$, Table 7). The extremely weak correlation between DO and ebullition was also seen in Ortega et al. (2019). This weak correlation could be attributed to DO in the water column not being a good indicator of oxygen content in the porewater of the sediment.

Linear regression analysis did not provide evidence that conductivity was a driver of ebullition differences amongst ponds (Table 8), whereas Kendall correlations indicated a significant positive correlation between ebullition and conductivity over time ($p < .0001$; Table

7). A positive correlation was not what was as expected, since rising salinity has been shown to decrease CH_4 emissions (Denier van der Gon & Neue, 1995). However, this positive correlation likely had more to do with the seasonality of both ebullition and conductivity, where both ebullition and conductivity decreased from summer to autumn ($p < .0001$, Table 2b). Salinity, and thus conductivity, spikes during months road salt is applied and declines once road salt application stops (Scott, 1981). Thus, it was expected that conductivity decreased from June to October in our study.

Further investigation into land cover adjacent to the ponds could help to determine drivers of CH_4 emissions. The surrounding land cover varied greatly in our study, some stormwater ponds were in the center of green space whereas others were connected to forested land. Differences in land use and cover influences aquatic ecosystem characteristics that are known to impact CH_4 emissions, including nutrient levels (Vaughan et al., 2017) and OM (Mitrovic & Baldwin, 2016). OM had a clear relationship with CH_4 production potential in our study, but it did not have as clear of a relationship with CH_4 ebullition. Egret and Redbridge had high levels of OM and high ebullition, and Martin had low OM and low ebullition, which coincides with what has been seen in literature, where OM positively correlates with CH_4 emissions (Kelly & Chynoweth, 1981). However, the fact that S Lot had low OM but high ebullition indicates that shallow stormwater ponds do not necessarily need high levels of OM to have high fluxes of CH_4.

The ponds with the highest production potential also had the highest oxidation potential. This was as expected since CH_4 feeds methane oxidation. However, since ponds from our study were shallow, with average pond depth less than 1m, additional CH_4 oxidation as CH_4 moved through the water column was likely limited, since there was little interaction with the water

column, as described by (Holgerson & Raymond, 2016). This would result in an increase in diffusive emissions, since bubble flux already escapes interaction with the water column. Unexpectedly, we see low diffusive flux in our study, especially compared to what has been seen from stormwater ponds throughout literature (Herrero Ortega et al., 2019; van Bergen et al., 2019).

Aeration was predicted to decrease CH_4 flux through increasing CH_4 oxidation, however, this was difficult to assess in this study. Only two of the eight ponds in our study had aeration systems and one of them was Martin, which had extremely low emissions and other management techniques were being utilized. Because of this, it did not seem appropriate to compare CH_4 fluxes between aerated and non-aerated ponds. Additionally, DO in aerated ponds was not higher than in non-aerated ponds, indicating that aeration may not have influence methane oxidation as originally hypothesized.

The presence of submerged plants could have altered the degree of CH_4 oxidation and production in each pond. Roots from submerged vegetation can increase oxidation and decrease production through the delivery of oxygen from their roots to the sediment (Bastviken, 2019). J Lot had noticeable submerged and rooted vegetation including pondweed (*Potamogeton* sp.), while CH_4 flux from J Lot was also relatively low (Table 4 and Table 5). Redbridge had noticeable submerged vegetation but very high CH_4 flux. However, this could be due to the non-rooted nature of the macroalgae, stonewort (*Chara* sp.). Vegetation surveys of submerged vegetation in stormwater ponds instead of purely qualitative descriptions could have helped identify the impact of submerged vegetation on CH_4 fluxes from stormwater ponds.

Management could have influenced CH_4 emissions from our stormwater ponds. The use of algaecide, such as the copper-based algaecide used at Martin, has the potential to decrease

CH_4 emissions due to known linkages between primary production and methanogenesis. Copper has also been shown to significantly stunt microbial methane production (Ahring & Westermann, 1985; Hobson & Shaw, 1976; Karri, Sierra-Alvarez, & Field, 2006), where road debris contributes to the heavy metal contamination in stormwater ponds. Data from Lusk & Chapman (2020) illustrates that the use of copper algaecide in stormwater ponds leads to significant copper concentrations in the water column, sediment and plant tissue. We did not directly assess the concentration of copper, however, knowledge of copper-based algicide use at Martin coupled with extremely low CH_4 emissions suggests a need for further investigation of algaecide impacts on CH_4 emissions in stormwater ponds. The benthic barrier installed at Tinker could also have impacted the magnitude of CH_4 emissions. Field observations showed that the benthic barrier at Tinker was trapping gas near the sediment, an observation that has also been documented in other studies (Gunnison & Barko, 1992). This may have contributed to the low CH_4 flux measured at Tinker. Benthic barriers may alter CH_4 emissions, by changing sediment conditions such as OM deposition to the sediment and by impacting rates and pathways of CH_4 transport. More research is needed on how benthic barriers affect CH_4 emissions from stormwater ponds.

5.5 Best management practices

Information gathered from our study and past studies provides insight on best management practices (BMPs) in limiting CH_4 emissions from stormwater ponds. Depth was a clear factor in influencing CH_4 emissions in our study, where both Kendall correlations and linear regression provide evidence that increasing depth decreases CH_4 emissions (Table 7 and Table 8). However, shallower stormwater ponds limit downstream pollution by reducing nitrogen levels than deeper ponds (Koch, Febria, Gevrey, Wainger, & Palmer, 2014), where New

York State has recommended that no stormwater pond has a maximum depth over 8 feet deep (Nysdec, 2010). Thus, increasing water depth in stormwater ponds may not be the most beneficial strategy overall. Reducing nutrient loading in aquatic ecosystems, however, has the double benefit of increasing water quality and potentially reducing CH_4 emissions. This can be seen in our study, where ponds with the highest TIN also had the highest CH_4 flux. Past studies also show this positive effect nutrients have on CH_4 emissions in urban aquatic ecosystems (Beaulieu et al., 2019; Davidson et al., 2015; Peacock et al., 2019; Sepulveda-Jauregui et al., 2018). Peacock et al. (2019) found that high nutrient ponds as determined by phosphorus concentrations resulted in increased CH_4 emissions. Additionally, in Mexico City, the CH_4 footprint per unit area for urban aquatic ecosystems was eight times higher than from Berlin, where temperature differences between the two cities likely only accounted for a 2-3x difference (Herrero Ortega et al., 2019). However, in Mexico City there are much fewer regulations on wastewater compared to Berlin, contributing to high nutrient inputs and hypereutrophic conditions into stormwater (Martinez-Cruz et al., 2017). Thus, it is imperative for municipalities to regulate nutrient inputs to stormwater ponds.

6.0 Conclusion

This dataset is a one of few that uses long-term and high frequency (N = 2030) methods to capture the extreme spatiotemporal and episodic variability of ebullition and is one of only a couple to do so for stormwater ponds. Continuous ebullitive flux collection spanned 140 days in 2019 and 98 days in 2020, much higher than the 39 days needed to accurately estimate CH_4 emissions determined by Wik et al. (2016). Additionally, the inverted funnel method used in our study increased accuracy by accounting for diurnal variations (Bastviken et al., 2004; Saunois et

al., 2016). Our data shows that CH_4 emissions from stormwater ponds in Rochester, NY were significant sources of greenhouse gas emissions to the atmosphere, similar to findings from other literature reported (Herrero Ortega et al., 2019; van Bergen et al., 2019). Trends from depth and nutrient status provided evidence that they were drivers in CH_4 emissions amongst ponds.

References:

Aben, R. C. H., Barros, N., Van Donk, E., Frenken, T., Hilt, S., Kazanjian, G., … Kosten, S. (2017). Cross continental increase in methane ebullition under climate change. *Nature Communications*, *8*(1), 1–8. https://doi.org/10.1038/s41467-017-01535-y

Ahring, B. K., & Westermann, P. (1985). Sensitivity of thermophilic methanogenic bacteria to heavy metals. *Current Microbiology*, *12*(5), 273–276. https://doi.org/10.1007/BF01567977

Armstrong, R. A. (2014, September 1). When to use the Bonferroni correction. *Ophthalmic & Physiological Optics : The Journal of the British College of Ophthalmic Opticians (Optometrists)*. John Wiley & Sons, Ltd. https://doi.org/10.1111/opo.12131

Auer, M. T., Kieser, M. S., & Canale, R. P. (1986). Identification of critical nutrient levels through field verification of models for phosphorus and phytoplankton growth. *Canadian Journal of Fisheries and Aquatic Sciences*, *43*(2), 379–388. https://doi.org/10.1139/f86-048

Avery, G. B., & Martens, C. S. (1999). Controls on the stable carbon isotopic composition of biogenic methane produced in a tidal freshwater estaurine sediment. *Geochimica et Cosmochimica Acta*, *63*(7–8), 1075–1082. https://doi.org/10.1016/S0016-7037(98)00315-9

Bailey, J., & Calhoun, J. K. (2008). Comparison of three physical management tchniques for controlling Variable-leaf Milfoil in Maine Lakes. *Journal of Aquatic Plant Management*, *46*, 163–167. Retrieved from http://www.maine.gov/dep/blwq/topic/inva-

Barker, H. A. (1936). On the biochemistry of the methane fermentation. *Archiv Für Mikrobiologie*, *7*(1–5), 404–419. https://doi.org/10.1007/BF00407413

Bastviken, D. (2009). Methane. In *Encyclopedia of Inland Waters* (2nd ed., pp. 783–805). Elsevier.

Bastviken, D., Cole, J. J., Pace, M. L., & Van de-Bogert, M. C. (2008). Fates of methane from different lake habitats: Connecting whole-lake budgets and CH4 emissions. *Journal of Geophysical Research: Biogeosciences*, *113*(2), 2024. https://doi.org/10.1029/2007JG000608

Bastviken, D., Cole, J., Pace, M., & Tranvik, L. (2004). Methane emissions from lakes: Dependence of lake characteristics, two regional assessments, and a global estimate. *Global Biogeochemical Cycles*, *18*(4), 1–12. https://doi.org/10.1029/2004GB002238

Bastviken, D., Santoro, A. L., Marotta, H., Pinho, L. Q., Calheiros, D. F., Crill, P., & Enrich-Prast, A. (2010). Methane emissions from pantanal, South America, during the low water season: Toward more comprehensive sampling. *Environmental Science and Technology*, *44*(14), 5450–5455. https://doi.org/10.1021/es1005048

Bastviken, D., Tranvik, L. J., Downing, J. A., Crill, P. M., & Enrich-Prast, A. (2011). Freshwater methane emissions offset the continental carbon sink. *Science*, *331*(6013), 50. https://doi.org/10.1126/science.1196808

Beaulieu, J., DelSontro, T., & Downing, J. (2019). Eutrophication will increase methane emissions from lakes and impoundments during the 21st century. *Nature Communications*, *10*(1). https://doi.org/10.1038/s41467-019-09100-5

Blaszczak, J. R., Steele, M. K., Badgley, B. D., Heffernan, J. B., Hobbie, S. E., Morse, J. L., … Bernhardt, E. S. (2018). Sediment chemistry of urban stormwater ponds and controls on denitrification. *Ecosphere*, *9*(6), e02318. https://doi.org/10.1002/ecs2.2318

Bocquier, P. (2005). *World urbanization prospects: An alternative to the UN model of projection compatible with the mobility transition theory*. *Demographic Research* (Vol. 12). https://doi.org/10.4054/DemRes.2005.12.9

Boon, P. I., & Mitchell, A. (1995). *Methanogenesis in the sediments of an Australian freshwater*

wetland: Comparison with aerobic decay, and factors controlling methanogenesis. *FEMS Microbiology Ecology* (Vol. 18). https://doi.org/10.1016/0168-6496(95)00053-5

Bricker, S. B., Longstaff, B., Dennison, W., Jones, A., Boicourt, K., Wicks, C., & Woerner, J. (2008). Effects of nutrient enrichment in the nation's estuaries: A decade of change. *Harmful Algae*, *8*(1), 21–32. https://doi.org/10.1016/j.hal.2008.08.028

Burke, S. A., Wik, M., Lang, A., Contosta, A. R., Palace, M., Crill, P. M., & Varner, R. K. (2019). Long-Term Measurements of Methane Ebullition From Thaw Ponds. *Journal of Geophysical Research: Biogeosciences*, *124*(7), 2208–2221. https://doi.org/10.1029/2018JG004786

Cao, M., Gregson, K., & Marshall, S. (1998). Global methane emission from wetlands and its sensitivity to climate change. *Atmospheric Environment*, *32*(19), 3293–3299. https://doi.org/10.1016/S1352-2310(98)00105-8

Carlson, R. E. (1977). A trophic state index for lakes. *Limnology and Oceanography*, *22*(2), 361–369. https://doi.org/10.4319/lo.1977.22.2.0361

Carpenter, S. R. (2005). Eutrophication of aquatic ecosystems: Bistability and soil phosphorus. *Proceedings of the National Academy of Sciences of the United States of America*, *102*(29), 10002–10005. https://doi.org/10.1073/pnas.0503959102

Casper, P., Maberly, S. C., Hall, G. H., & Finlay, B. J. (2000). *Fluxes of methane and carbon dioxide from a small productive lake to the atmosphere*. *Biogeochemistry* (Vol. 49). https://doi.org/10.1023/A:1006269900174

Chanton, J., Chaser, L., Glasser, P., & Siegel, D. (2005). *Carbon and Hydrogen Isotopic Effects in Microbial, Methane from Terrestrial Environments*. *Stable Isotopes and Biosphere - Atmosphere Interactions*. https://doi.org/10.1016/B978-012088447-6/50006-4

Chanton, J. P., & Martens, C. S. (1988). *Seasonal variations in ebullitive flux and carbon isotopic composition of methane in a tidal freshwater estuary*. *Global Biogeochemical Cycles* (Vol. 2). https://doi.org/10.1029/GB002i003p00289

Chanton, J. P., Martens, C. S., & Kelley, C. A. (1989). Gas transport from methane-saturated, tidal freshwater and wetland sediments. *Limnology and Oceanography*, *34*(5), 807–819. https://doi.org/10.4319/lo.1989.34.5.0807

Climate-Data. (2021). Average Temperature, weather by month, weather averages. Retrieved July 1, 2021, from https://en.climate-data.org/oceania/australia/victoria/ballarat-1795/%0Ahttps://en.climate-data.org/asia/thailand/bangkok/bangkok-6313/

Cohen, J. (2013). *Statistical Power Analysis for the Behavioral Sciences*. *Statistical Power Analysis for the Behavioral Sciences*. Routledge. https://doi.org/10.4324/9780203771587

Conrad, R. (2002). *Control of microbial methane production in wetland rice fields*. *Nutrient Cycling in Agroecosystems* (Vol. 64). https://doi.org/10.1023/A:1021178713988

Crawford, J. T., Stanley, E. H., Spawn, S. A., Finlay, J. C., Loken, L. C., & Striegl, R. G. (2014). Ebullitive methane emissions from oxygenated wetland streams. *Global Change Biology*, *20*(11), 3408–3422. https://doi.org/10.1111/gcb.12614

Davidson, T. A., Audet, J., Jeppesen, E., Landkildehus, F., Lauridsen, T. L., Søndergaard, M., & Syväranta, J. (2018). Synergy between nutrients and warming enhances methane ebullition from experimental lakes. *Nature Climate Change*, *8*, 156–160. https://doi.org/10.1038/s41558-017-0063-z

Davidson, T. A., Audet, J., Svenning, J. C., Lauridsen, T. L., Søndergaard, M., Landkildehus, F., … Jeppesen, E. (2015). Eutrophication effects on greenhouse gas fluxes from shallow-lake mesocosms override those of climate warming. *Global Change Biology*, *21*(12), 4449–

4463. https://doi.org/10.1111/gcb.13062
DelSontro, T., Beaulieu, J. J., & Downing, J. A. (2018). Greenhouse gas emissions from lakes and impoundments: Upscaling in the face of global change. *Limnology and Oceanography Letters*, *3*(3), 64–75. https://doi.org/10.1002/lol2.10073
DelSontro, T., Boutet, L., St-Pierre, A., del Giorgio, P. A., & Prairie, Y. T. (2016). Methane ebullition and diffusion from northern ponds and lakes regulated by the interaction between temperature and system productivity. *Limnology and Oceanography*, *61*(S1), S62–S77. https://doi.org/10.1002/lno.10335
Denier van der Gon, H. A. C., & Neue, H. U. (1995). Methane emission from a wetland rice field as affected by salinity. *Plant and Soil*, *170*(2), 307–313. https://doi.org/10.1007/BF00010483
Doane, T. A., & Horwáth, W. R. (2003). Spectrophotometric determination of nitrate with a single reagent. *Analytical Letters*, *36*(12), 2713–2722. https://doi.org/10.1081/AL-120024647
Duc, N. T., Crill, P., & Bastviken, D. (2010). Implications of temperature and sediment characteristics on methane formation and oxidation in lake sediments. *Biogeochemistry*, *100*(1), 185–196. https://doi.org/10.1007/s10533-010-9415-8
Environmental Protection Agency. (2009). *Stormwater Wet Pond and Wetland Management Guidebook*. *Center For Watershed Protection*. https://doi.org/10.1215/10474552-2009-007
EPA. Federal Water Pollution Control Act, As Amended by the Clean Water Act of 1987 (1987). Retrieved from https://www3.epa.gov/npdes/pubs/cwatxt.txt
EPA. (2009). Stormwater wet pond and wetland management guidebook. *Center For Watershed Protection*, 80. Retrieved from www.stormwatercenter.net
EPA. (2016). Indicators: Dissolved Oxygen | National Aquatic Resource Surveys | US EPA. Retrieved July 12, 2021, from https://bit.ly/3vWIbEQ
Feng, K., Guo, J. L., Chen, C., Wang, W., & Du, R. W. (2013). *Study on preservation and restoration for traditional dwellings in different historical periods*. *Applied Mechanics and Materials* (Vol. 368–370). https://doi.org/10.4028/www.scientific.net/AMM.368-370.99
Foster, I. (1994). *Restoration and management of lakes and reservoirs (2nd edn), edited by G. Dennis Cooke, Eugene B. Welch, Spencer A. Peterson and Peter R. Newroth, Lewis Publishers, CRC Press, Boca Raton. No. of pages: 548. price: £56.00. ISBN 0 87371 397 4*. *Regulated Rivers: Research & Management* (3rd ed., Vol. 9). Boca Raton: Taylor and Francis Group. https://doi.org/10.1002/rrr.3450090207
Gensemer, R., Canton, S., DeJong, G., Wolf, C., & Claytor, C. (2011). Should there be an aquatic life water quality criterion for conductivity? *SME Annual Meeting and Exhibit and CMA 113th National Western Mining Conference 2011*, 363–370. https://doi.org/10.2175/193864711802864714
Gorsky, A. L., Racanelli, G. A., Belvin, A. C., & Chambers, R. M. (2019). Greenhouse gas flux from stormwater ponds in southeastern Virginia (USA). *Anthropocene*, *28*, 100218. https://doi.org/10.1016/j.ancene.2019.100218
Grossart, H.-P., Frindte, K., Dziallas, C., Eckert, W., & Tang, K. W. (2011). Microbial methane production in oxygenated water column of an oligotrophic lake. *Proceedings of the National Academy of Sciences*, *108*(49), 19657–19661. https://doi.org/10.1073/PNAS.1110716108
Guérin, F., & Abril, G. (2007). Significance of pelagic aerobic methane oxidation in the methane and carbon budget of a tropical reservoir. *Journal of Geophysical Research:*

Biogeosciences, *112*(3), n/a-n/a. https://doi.org/10.1029/2006JG000393
Gunnison, D., & Barko, J. W. (1992). Factors Influencing Gas Evolution Beneath a Benthic Barrier. *Journal of Aquatic Plant Management*, *30*, 23–28.
Hein, R., Crutzen, P. J., & Heimann, M. (1997). An inverse modeling approach to investigate the global atmospheric methane cycle. *Global Biogeochemical Cycles*, *11*(1), 43–76. https://doi.org/10.1029/96GB03043
Heiri, O., Lotter, A. F., & Lemcke, G. (2001). Loss on ignition as a method for estimating organic and carbonate content in sediments: reproducibility and comparability of results. *Journal of Paleolimnology*, *25*(1), 101–110. https://doi.org/10.1023/A:1008119611481
Herb, W. R., Mohseni, O., & Stefan, H. G. (2009). *Simulation of Temperature Mitigation by a Stormwater Detention Pond1*. *Journal of the American Water Resources Association* (Vol. 45). https://doi.org/10.1111/j.1752-1688.2009.00354.x
Herrero Ortega, S., Romero González-Quijano, C., Casper, P., Singer, G. A., & Gessner, M. O. (2019). Methane emissions from contrasting urban freshwaters: Rates, drivers, and a whole-city footprint. *Global Change Biology*, *25*(12), 4234–4243. https://doi.org/10.1111/gcb.14799
Hobson, P. N., & Shaw, B. G. (1976). Inhibition of methane production by Methanobacterium formicicum. *Water Research*, *10*(10), 849–852. https://doi.org/10.1016/0043-1354(76)90018-X
Hodgkins, S. B., Tfaily, M. M., McCalley, C. K., Logan, T. A., Crill, P. M., Saleska, S. R., … Chanton, J. P. (2014). Changes in peat chemistry associated with permafrost thaw increase greenhouse gas production. *Proceedings of the National Academy of Sciences of the United States of America*, *111*(16), 5819–5824. https://doi.org/10.1073/pnas.1314641111
Holgerson, M. A., & Raymond, P. A. (2016). Large contribution to inland water CO2 and CH4 emissions from very small ponds. *Nature Geoscience*, *9*(3), 222–226. https://doi.org/10.1038/ngeo2654
IPCC. (2018). *IPCC Special Report on the impacts of global warming of 1.5°C*. *Ipcc - Sr15*. Retrieved from https://report.ipcc.ch/sr15/pdf/sr15_spm_final.pdf%0Ahttp://www.ipcc.ch/report/sr15/
Ivanovsky, A., Belles, A., Criquet, J., Dumoulin, D., Noble, P., Alary, C., & Billon, G. (2018). Assessment of the treatment efficiency of an urban stormwater pond and its impact on the natural downstream watercourse. *Journal of Environmental Management*, *226*, 120–130. https://doi.org/10.1016/j.jenvman.2018.08.015
Jędrysek, M. O. (1999). Spatial and temporal patterns in diurnal variations of carbon isotope ratios of early-diagenetic methane from freshwater sediments. *Chemical Geology*, *159*(1–4), 241–262. https://doi.org/10.1016/S0009-2541(99)00040-6
Karri, S., Sierra-Alvarez, R., & Field, J. A. (2006). Toxicity of copper to acetoclastic and hydrogenotrophic activities of methanogens and sulfate reducers in anaerobic sludge. *Chemosphere*, *62*(1), 121–127. https://doi.org/10.1016/j.chemosphere.2005.04.016
Kaushal, S. S., Groffman, P. M., Likens, G. E., Belt, K. T., Stack, W. P., Kelly, V. R., … Fisher, G. T. (2005). Increased salinization of fresh water in the Northeastern United States. *Proceedings of the National Academy of Sciences of the United States of America*, *102*(38), 13517–13520. https://doi.org/10.1073/pnas.0506414102
Kavehei, E., Jenkins, G. A., Adame, M. F., & Lemckert, C. (2018). Carbon sequestration potential for mitigating the carbon footprint of green stormwater infrastructure. *Renewable and Sustainable Energy Reviews*, *94*, 1179–1191. https://doi.org/10.1016/j.rser.2018.07.002

Kelly, C. A., & Chynoweth, D. P. (1981). The contributions of temperature and of the input of organic matter in controlling rates of sediment methanogenesis. *Limnology and Oceanography*, *26*(5), 891–897. https://doi.org/10.4319/lo.1981.26.5.0891

King, G. M. (1990). Dynamics and controls of methane oxidation in a Danish wetland sediment. *FEMS Microbiology Letters*, *74*(4), 309–323. https://doi.org/10.1111/j.1574-6968.1990.tb04078.x

Kirschke, S., Bousquet, P., Ciais, P., Saunois, M., Canadell, J. G., Dlugokencky, E. J., … Zeng, G. (2013). Three decades of global methane sources and sinks. *Nature Geoscience*, *6*(10), 813–823. https://doi.org/10.1038/ngeo1955

Koch, B. J., Febria, C. M., Gevrey, M., Wainger, L. A., & Palmer, M. A. (2014). Nitrogen Removal by Stormwater Management Structures: A Data Synthesis. *Journal of the American Water Resources Association*, *50*(6), 1594–1607. https://doi.org/10.1111/jawr.12223

Kratzer, C. R., & Brezonik, P. L. (1981). a Carlson-Type Trophic State Index for Nitrogen in Florida Lakes. *JAWRA Journal of the American Water Resources Association*, *17*(4), 713–715. https://doi.org/10.1111/j.1752-1688.1981.tb01282.x

Larmola, T., Tuittila, E.-S., Tiirola, M., Nykänen, H., Martikainen, P. J., Yrjälä, K., … Fritze, H. (2010). The role of *Sphagnum* mosses in the methane cycling of a boreal mire. *Ecology*, *91*(8), 2356–2365. https://doi.org/10.1890/09-1343.1

Lusk, M. G., & Chapman, K. (2020). Copper concentration data for water, sediments, and vegetation of urban stormwater ponds treated with copper sulfate algaecide. *Data in Brief*, *31*, 105982. https://doi.org/10.1016/J.DIB.2020.105982

MacPherson, T. A., Cahoon, L. B., & Mallin, M. A. (2007). Water column oxygen demand and sediment oxygen flux: patterns of oxygen depletion in tidal creeks. *Hydrobiologia 2007 586:1*, *586*(1), 235–248. https://doi.org/10.1007/S10750-007-0643-4

Marsalek, J. (2003). Road salts in urban stormwater: An emerging issue in stormwater management in cold climates. In *Water Science and Technology* (Vol. 48, pp. 61–70). https://doi.org/10.2166/wst.2003.0493

Martinez-Cruz, K., Gonzalez-Valencia, R., Sepulveda-Jauregui, A., Plascencia-Hernandez, F., Belmonte-Izquierdo, Y., & Thalasso, F. (2017). Methane emission from aquatic ecosystems of Mexico City. *Aquatic Sciences*, *79*(1), 159–169. https://doi.org/10.1007/s00027-016-0487-y

Mattson, M. D., & Likens, G. E. (1990). Air pressure and methane fluxes [8]. *Nature*, *347*(6295), 718–719. https://doi.org/10.1038/347718b0

Maynard, D. G., Kalra, Y. P., & Crumbaugh, J. A. (1993). *Nitrate and exchangeable ammonium nitrogen. In M. R. Carter (Chapter 6), Soil sampling and methods of analysis*. (M. R. Carter, Ed.) (1st ed.). Boca Raton: Lewis Publishers.

Mengel, K., & Kirkby, E. A. (2001). *Principles of Plant Nutrition*. *Principles of Plant Nutrition* (5th ed.). Dordrecht: Kluwer Academic Publishers. https://doi.org/10.1007/978-94-010-1009-2

Mitchell, B. D., & Richards, K. (1992). Macroinvertebrate communities in two salt affected tributaries of the Hopkins Rives, Victoria. *International Journal of Salt Lake Research*, *1*(1), 81–102. https://doi.org/10.1007/BF02904953

Mitrovic, S. M., & Baldwin, D. S. (2016). Allochthonous dissolved organic carbon in river, lake and coastal systems: Transport, function and ecological role. *Marine and Freshwater Research*, *67*(9), i–iv. https://doi.org/10.1071/MFv67n9_ED

Moore, T. L. C., & Hunt, W. F. (2013). Predicting the carbon footprint of urban stormwater infrastructure. *Ecological Engineering*, *58*, 44–51. https://doi.org/10.1016/j.ecoleng.2013.06.021

Murphy, J., & Riley, J. P. (1962). *A modified single solution method for the determination of phosphate in natural waters*. *Analytica Chimica Acta* (Vol. 27). https://doi.org/10.1016/S0003-2670(00)88444-5

Natchimuthu, S., Panneer Selvam, B., & Bastviken, D. (2014). Influence of weather variables on methane and carbon dioxide flux from a shallow pond. *Biogeochemistry*, *119*(1–3), 403–413. https://doi.org/10.1007/s10533-014-9976-z

Nielsen, S. S. (1998). *Pigment Analysis*. *Instructor's Manual for Food Analysis: Second Edition* (2nd ed.). Ottawa: Fisheries Research Board of Canada. https://doi.org/10.1007/978-1-4615-5439-4_19

Nysdec. (2010). *New York State Stormwater Management Design Manual*.

Peacock, M., Audet, J., Jordan, S., Smeds, J., & Wallin, M. B. (2019). Greenhouse gas emissions from urban ponds are driven by nutrient status and hydrology. *Ecosphere*, *10*(3), e02643. https://doi.org/10.1002/ecs2.2643

Peixoto, R., Machado-Silva, F., Marotta, H., Enrich-Prast, A., & Bastviken, D. (2015). Spatial versus Day-To-Day Within-Lake Variability in Tropical Floodplain Lake CH4 Emissions - Developing Optimized Approaches to Represent Flux Measurements. *PLoS ONE*, *10*(4).

Poissant, L., Constant, P., Pilote, M., Canário, J., O'Driscoll, N., Ridal, J., & Lean, D. (2007). The ebullition of hydrogen, carbon monoxide, methane, carbon dioxide and total gaseous mercury from the Cornwall Area of Concern. *Science of the Total Environment*, *381*(1–3), 256–262. https://doi.org/10.1016/j.scitotenv.2007.03.029

Rochester, NY Weather History | Weather Underground. (n.d.). Retrieved July 28, 2021, from https://www.wunderground.com/history/daily/KROC

Sabouri, F., Gharabaghi, B., Mahboubi, A. A., & McBean, E. A. (2013). Impervious surfaces and sewer pipe effects on stormwater runoff temperature. *Journal of Hydrology*, *502*, 10–17. https://doi.org/10.1016/j.jhydrol.2013.08.016

Saulnier-Talbot, É., & Lavoie, I. (2018). Uncharted waters: the rise of human-made aquatic environments in the age of the "Anthropocene." *Anthropocene*, *23*, 29–42. https://doi.org/10.1016/j.ancene.2018.07.003

Saunois, M., Bousquet, P., Poulter, B., Peregon, A., Ciais, P., Canadell, J. G., … Zhu, Q. (2016). The global methane budget 2000-2012. *Earth System Science Data*, *8*(2), 697–751. https://doi.org/10.5194/essd-8-697-2016

Scandella, B. P., Varadharajan, C., Hemond, H. F., Ruppel, C., & Juanes, R. (2011). A conduit dilation model of methane venting from lake sediments. *Geophysical Research Letters*, *38*(6). https://doi.org/10.1029/2011GL046768

Schindler, D. W. (1977). Evolution of phosphorus limitation in lakes. *Science*, *195*(4275), 260–262. https://doi.org/10.1126/science.195.4275.260

Schueler, T. R. (1987). *Controlling Urban Runoff: A Practical Manual for Planning and Designing Urban BMPs*. Washington, D.C.: Metropolitan Information Center. https://doi.org/10.1016/S1251-8050(00)00231-7

Scott, W. S. (1981). An analysis of factors influencing de-icing salt levels in streams. *Journal of Environmental Management*, *13*(3), 269–287.

Sepulveda-Jauregui, A., Hoyos-Santillan, J., Martinez-Cruz, K., Walter Anthony, K. M., Casper, P., Belmonte-Izquierdo, Y., & Thalasso, F. (2018). Eutrophication exacerbates the impact

of climate warming on lake methane emission. *Science of the Total Environment*, *636*, 411–419. https://doi.org/10.1016/j.scitotenv.2018.04.283
Smith, L. K., & Lewis, W. M. (1992). Seasonality of methane emissions from five lakes and associated wetlands of the Colorado Rockies. *Global Biogeochemical Cycles*, *6*(4), 323–338. https://doi.org/10.1029/92GB02016
SOLÓRZANO, L. (1969). DETERMINATION OF AMMONIA IN NATURAL WATERS BY THE PHENOLHYPOCHLORITE METHOD 1 1 This research was fully supported by U.S. Atomic Energy Commission Contract No. ATS (11-1) GEN 10, P.A. 20. *Limnology and Oceanography*, *14*(5), 799–801. https://doi.org/10.4319/lo.1969.14.5.0799
Takai, Y. (1970). The mechanism of methane fermentation in flooded paddy soil. *Soil Science and Plant Nutrition*, *16*(6), 238–244. https://doi.org/10.1080/00380768.1970.10433371
US Department of Commerce, N. N. W. S. (n.d.). Rochester Climate Narrative.
van Bergen, T. J. H. M., Barros, N., Mendonça, R., Aben, R. C. H., Althuizen, I. H. J., Huszar, V., … Kosten, S. (2019). Seasonal and diel variation in greenhouse gas emissions from an urban pond and its major drivers. *Limnology and Oceanography*, *64*(5), 2129–2139. https://doi.org/10.1002/lno.11173
van der Gon, H. A. C. D., & Neue, H. U. (1995). Methane emission from a wetland rice field as affected by salinity. *Plant and Soil*, *170*(2), 307–313. https://doi.org/10.1007/BF00010483
Van Hulzen, J. B., Segers, R., Van Bodegom, P. M., & Leffelaar, P. A. (1999). Temperature effects on soil methane production: An explanation for observed variability. *Soil Biology and Biochemistry*, *31*(14), 1919–1929. https://doi.org/10.1016/S0038-0717(99)00109-1
Vaughan, M. C. H., Bowden, W. B., Shanley, J. B., Vermilyea, A., Sleeper, R., Gold, A. J., … Schroth, A. W. (2017). High-frequency dissolved organic carbon and nitrate measurements reveal differences in storm hysteresis and loading in relation to land cover and seasonality. *Water Resources Research*, *53*(7), 5345–5363. https://doi.org/10.1002/2017WR020491
Waajen, G. W. A. M., Faassen, E. J., & Lürling, M. (2014). Eutrophic urban ponds suffer from cyanobacterial blooms: Dutch examples. *Environmental Science and Pollution Research*, *21*(16), 9983–9994. https://doi.org/10.1007/s11356-014-2948-y
West, W. E., Creamer, K. P., & Jones, S. E. (2016). Productivity and depth regulate lake contributions to atmospheric methane. *Limnology and Oceanography*, *61*, S51–S61. https://doi.org/10.1002/lno.10247
Whalen, S. C. (2005). *Biogeochemistry of methane exchange between natural wetlands and the atmosphere*. *Environmental Engineering Science* (Vol. 22). https://doi.org/10.1089/ees.2005.22.73
Wik, M., Crill, P. M., Varner, R. K., & Bastviken, D. (2013). Multiyear measurements of ebullitive methane flux from three subarctic lakes. *Journal of Geophysical Research: Biogeosciences*, *118*(3), 1307–1321. https://doi.org/10.1002/jgrg.20103
Wik, M., Thornton, B. F., Bastviken, D., Uhlbäck, J., & Crill, P. M. (2016). Biased sampling of methane release from northern lakes: A problem for extrapolation. *Geophysical Research Letters*, *43*(3), 1256–1262. https://doi.org/10.1002/2015GL066501
Williams, C. J., Frost, P. C., Morales-Williams, A. M., Larson, J. H., Richardson, W. B., Chiandet, A. S., & Xenopoulos, M. A. (2016). Human activities cause distinct dissolved organic matter composition across freshwater ecosystems. *Global Change Biology*, *22*(2), 613–626. https://doi.org/10.1111/gcb.13094
Woltemate, I., Whiticar, M. J., & Schoell, M. (1984). Carbon and hydrogen isotopic composition of bacterial methane in a shallow freshwater lake. *Limnology and Oceanography*, *29*(5),

985–992. https://doi.org/10.4319/lo.1984.29.5.0985
Xing, Y., Xie, P., Yang, H., Ni, L., Wang, Y., & Rong, K. (2005). Methane and carbon dioxide fluxes from a shallow hypereutrophic subtropical Lake in China. *Atmospheric Environment*, *39*(30), 5532–5540. https://doi.org/10.1016/j.atmosenv.2005.06.010
Zhao, Q., Jia, X., Xia, R., Lin, J., & Zhang, Y. (2016). A field-based method to derive macroinvertebrate benchmark for specific conductivity adapted for small data sets and demonstrated in the Hun-Tai River Basin, Northeast China. *Environmental Pollution*, *216*, 902–910. https://doi.org/10.1016/j.envpol.2016.06.065

Tables and Figures

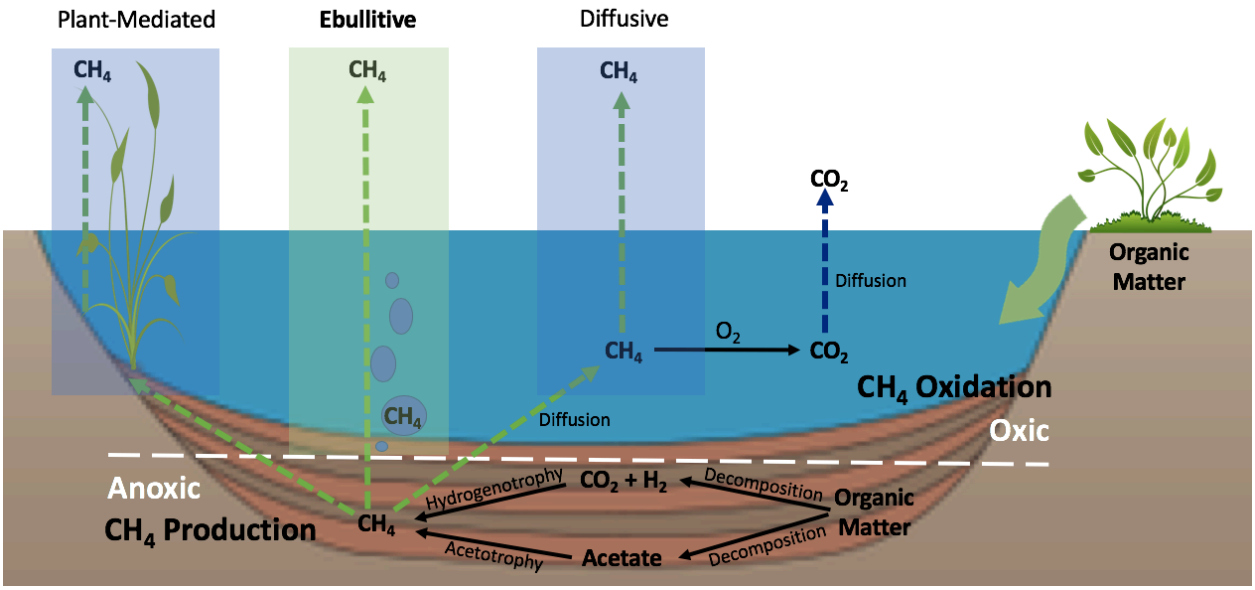

Figure 1. Carbon cycling and CH_4 flux pathways in a stormwater pond. The green dashed arrows indicate CH_4 flux pathways. The blue arrow indicates CO_2 diffusion as a result of methanotrophy. The black arrows indicate chemical reactions.

Table 1. Characteristics of all 8 stormwater ponds sampled across years. Differences in shading correspond to differences in years sampled.

Pond	Year Sampled	Catchment area	Max Depth (m)	Surface Area (m^2)	Year Built	Aeration
J Lot	2019 & 2020	RIT Campus	2.0	3120	2005	No
Egret	2019 & 2020	Residential	2.1	1660	2003	No
Redbridge	2019 & 2020	Residential	0.80	1130	2003	No
Nightfrost	2019	Residential	1.60	6470	2001	No
Tinker	2019	Park	2.2	4050	1996	No
Martin	2020	Park	3.7	4370	2002	Yes
D Lot	2020	RIT Campus	1.60	1050	2004	Yes
S Lot	2020	RIT Campus	0.8	1130	1998	No

Table 2a. Statistics included are 2-way ANOVAs examining water temperature, DO and conductivity with site and month. Bolded values indicate statistically significant *p* values. Nightfrost was not included in statistics.

	Site		Month		Site*Month	
	F	*p*	*F*	*p*	*F*	*p*
Water Temp (°C)	$F_{6,1728} = 85.6$	**< .0001**	$F_{4,1728} = 1840$	**< .0001**	$F_{19,1728} = 8.64$	**< .0001**
DO (mg/L)	$F_{6,1728} = 113$	**< .0001**	$F_{4,1728} = 19.8$	**< .0001**	$F_{19,1728} = 10.4$	**< .0001**
Conductivity (µS/cm)	$F_{6,1728} = 933$	**< .0001**	$F_{4,1728} = 213$	**< .0001**	$F_{19,1728} = 29.5$	**< .0001**

Table 2b. Water temperature, DO and conductivity (avg ± SE). Tukey HSD results are shown in superscripts. Tukey results are displayed in superscripts and are based on the two-way ANOVA results from Table 2a.

	Water Temperature (°C)	DO (mg /L)	Conductivity (µS /cm)
D Lot	$19.8 \pm 0.375^{\mathbf{d}}$	$10.6 \pm 0.109^{\mathbf{b}}$	$599 \pm 7.89^{\mathbf{c}}$
Egret	$20.3 \pm 0.196^{\mathbf{d}}$	$5.31 \pm 0.271^{\mathbf{e}}$	$487 \pm 5.85^{\mathbf{d}}$
J Lot	$21.9 \pm 0.227^{\mathbf{b}}$	$9.22 \pm 0.220^{\mathbf{c}}$	$1140 \pm 16.0^{\mathbf{a}}$
Martin	$22.3 \pm 0.389^{\mathbf{b}}$	$7.03 \pm 0.170^{\mathbf{d}}$	$438 \pm 3.11^{\mathbf{e}}$
Nightfrost	22.8 ± 0.153	4.86 ± 0.257	781 ± 9.33
Redbridge	$20.8 \pm 0.231^{\mathbf{c}}$	$11.6 \pm 0.354^{\mathbf{b}}$	$725 \pm 7.62^{\mathbf{b}}$
S Lot	$23.8 \pm 0.440^{\mathbf{a}}$	$14.9 \pm 0.343^{\mathbf{a}}$	$1170 \pm 29.0^{\mathbf{a}}$
Tinker	$21.9 \pm 0.378^{\mathbf{b}}$	$8.15 \pm 0.241^{\mathbf{cd}}$	$634 \pm 4.65^{\mathbf{c}}$
June	$18.8 \pm 0.218^{\mathbf{d}}$	$6.37 \pm 0.645^{\mathbf{d}}$	$930 \pm 81.8^{\mathbf{a}}$
July	$25.2 \pm 0.111^{\mathbf{a}}$	$8.29 \pm 0.264^{\mathbf{c}}$	$874 \pm 16.4^{\mathbf{a}}$
August	$23.8 \pm 0.0823^{\mathbf{b}}$	$8.62 \pm 0.235^{\mathbf{c}}$	$800 \pm 12.3^{\mathbf{b}}$
September	$20.4 \pm 0.107^{\mathbf{c}}$	$10.9 \pm 0.247^{\mathbf{a}}$	$747 \pm 13.5^{\mathbf{c}}$
October	$14.0 \pm 0.139^{\mathbf{e}}$	$9.81 \pm 0.216^{\mathbf{b}}$	$569 \pm 9.85^{\mathbf{d}}$

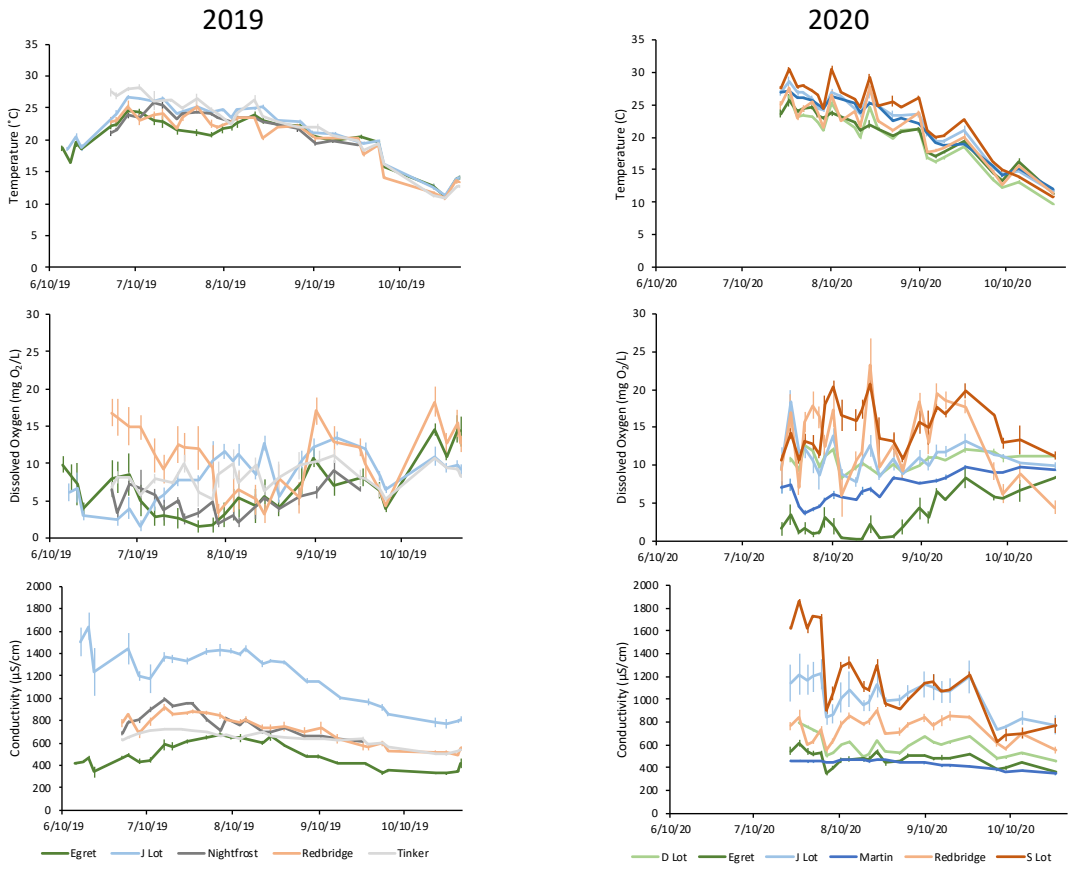

Figure 2. Water temperature, DO and conductivity (avg ± SE, n = 6-10) throughout time for 2019 and 2020.

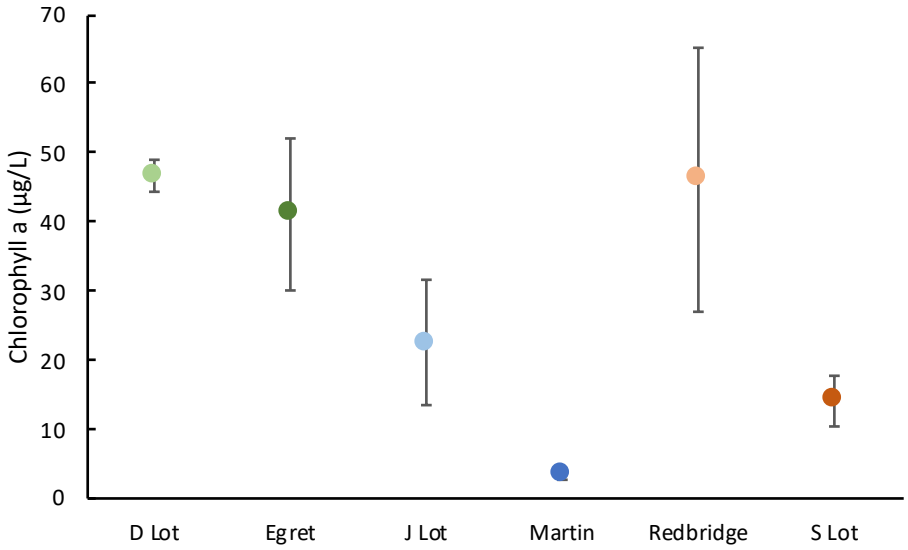

Figure 3. Chl *a* in µg/L (average ± SE, n = 4) for stormwater ponds. Water samples were collected on September 15th and 16th, 2020. Significant differences detected from a one-way ANOVA ($F_{5,24} = 3.39$, $p = .03$), however Tukey HSD did not output significant differences amongst ponds.

Table 3a. Results from two-way ANOVAs examining water column NO_3^-, NH_4^{3+}, TIN and PO_4^{3-} with site and season keeping years separate. Nightfrost was not included in the statistics since it does not have autumn water nutrient data.

		Site		Season		Site*Season	
		F	*p*	*F*	*p*	*F*	*p*
NO_3^-	2019	$F_{3,47}$=7.79	**< .001**	$F_{2,47}$=1.71	0.19	$F_{6,47}$=2.86	**.019**
	2020	$F_{5,89}$ = 8.55	**< .0001**	$F_{2,89}$ = 15.4	**< .0001**	$F_{10,89}$ = 6.54	**< .0001**
NH_4^+	2019	$F_{3,47}$ = 3.56	**.021**	$F_{2,47}$= 104	**< .0001**	$F_{6,47}$=2.31	**.049**
	2020	$F_{5,90}$ = 8.34	**< .0001**	$F_{2,90}$ = 9.37	**< .001**	$F_{10,90}$ = 4.99	**< .0001**
TIN	2019	$F_{3,47}$ =6.80	**< .001**	$F_{2,47}$ =20.3	**< .0001**	$F_{6,47}$ =2.44	**.039**
	2020	$F_{5,90}$ = 74.7	**< .0001**	$F_{2,90}$ = 128	**< .0001**	$F_{10,90}$ = 50.0	**< .0001**
PO_4^{3-}	2019	$F_{3,47}$ = 1.55	.21	$F_{2,47}$= 2.80	.071	$F_{6,47}$= 8.19	**< .0001**
	2020	$F_{5,90}$ = 107	**< .0001**	$F_{2,90}$ = 198	**< .0001**	$F_{10,90}$ = 53.5	**< .0001**

Table 3b. Water NO_3^-, NH_4^+, TIN and PO_4^{3-} concentrations per site and year displayed as average ± SE. Tukey results are displayed in superscripts and are based on the two-way ANOVA results from Table 3a.

		D Lot	Egret	J Lot	Martin	Nightfrost	Redbridge	S Lot	Tinker
$N\text{-}NO_3^-$ µg/L	2019	nd	18.7 ± 12.0$^{\mathbf{b}}$	0.799 ± 0.496$^{\mathbf{b}}$	nd	2.14 ± 1.23	110 ± 41.2$^{\mathbf{a}}$	nd	0.637 ± 0.318$^{\mathbf{b}}$
	2020	184 ± 37.8$^{\mathbf{ab}}$	77.6 ± 13.5$^{\mathbf{bc}}$	37.5 ± 18.0$^{\mathbf{c}}$	53.7 ± 26.3$^{\mathbf{bc}}$	nd	282 ± 109$^{\mathbf{a}}$	13.8 ± 4.48$^{\mathbf{c}}$	nd
$N\text{-}NH_4^+$ µg/L	2019	nd	52.8 ± 16.6$^{\mathbf{a}}$	49.0 ± 18.5$^{\mathbf{ab}}$	nd	9.08± 1.06	37.5 ± 11.7$^{\mathbf{ab}}$	nd	25.8 ± 8.36$^{\mathbf{b}}$
	2020	63.7 ± 5.11$^{\mathbf{b}}$	172 ± 38.8$^{\mathbf{b}}$	67.1 ± 6.50$^{\mathbf{b}}$	93.3 ± 7.10$^{\mathbf{b}}$	nd	374 ± 118$^{\mathbf{a}}$	97.2 ± 16.6$^{\mathbf{b}}$	nd
N-TIN µg/L	2019	nd	71.5 ± 18.4$^{\mathbf{b}}$	49.8 ± 18.7$^{\mathbf{b}}$	nd	10.3 ± 2.16	148 ± 48.8$^{\mathbf{a}}$	nd	26.5 ± 8.45$^{\mathbf{b}}$
	2020	248 ± 38.5$^{\mathbf{b}}$	250 ± 50.9$^{\mathbf{b}}$	105 ± 22.2$^{\mathbf{c}}$	147 ± 23.8$^{\mathbf{c}}$	nd	641 ± 147$^{\mathbf{a}}$	111 ± 18.4$^{\mathbf{c}}$	nd
$P\text{-}PO_4^{3-}$ µg/L	2019	nd	34.5 ± 4.39	40.8 ± 4.90	nd	45.8 ± 3.90	39.3 ± 3.17	nd	43.1 ± 3.18
	2020	8.00 ± 1.17$^{\mathbf{d}}$	42.4 ± 8.46$^{\mathbf{a}}$	7.15 ± 0.407$^{\mathbf{d}}$	31.2 ± 6.91$^{\mathbf{b}}$	nd	16.0 ± 1.87$^{\mathbf{c}}$	7.11 ± 5.32$^{\mathbf{d}}$	nd

Table 3c. NO_3^-, NH_4^+, TIN and PO_4^{3-} concentrations in (avg ± SE) per season. Tukey results are displayed in superscripts and are based on the two-way ANOVA results from Table 3a.

		Middle Summer	Late Summer	Autumn
$N\text{-}NO_3^-$ µg/L	2019	14.4 ± 9.66	28.6 ± 24.6	51.7 ± 22.7
	2020	63.6 ± 14.7^{b}	36.5 ± 13.7^{b}	218 ± 55.1^{a}
$N\text{-}NH_4^+$ µg/L	2019	11.0 ± 2.20^{b}	6.80 ± 0.980^{b}	110 ± 11.1^{a}
	2020	87.7 ± 9.85^{b}	98.7 ± 18.3^{b}	248 ± 63.2^{a}
N-TIN µg/L	2019	25.4± 9.98^{b}	35.4 ± 25.4^{b}	161 ± 20.3^{a}
	2020	150 ± 16.4^{b}	135 ± 20.8^{b}	466 ± 82.5^{a}
$P\text{-}PO_4^{3-}$ µg/L	2019	45.4 ± 4.26	38.0 ± 3.19	36.6 ± 2.50
	2020	34.9 ± 5.60^{a}	13.0 ± 1.65^{b}	8.02 ± 0.531^{c}

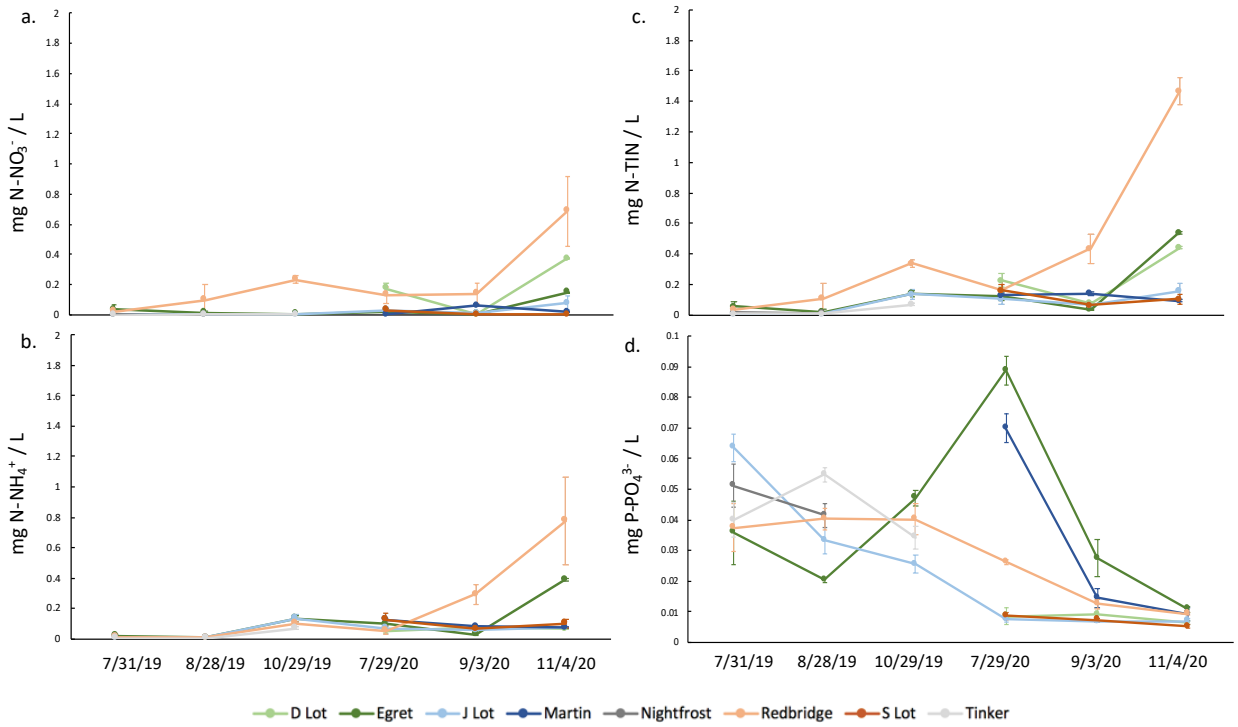

Figure 4. NO_3^-, NH_4^+, TIN and PO_4^{3+} (average ± SE,n = 5-6) from stormwater ponds across the 6 water sampling dates.

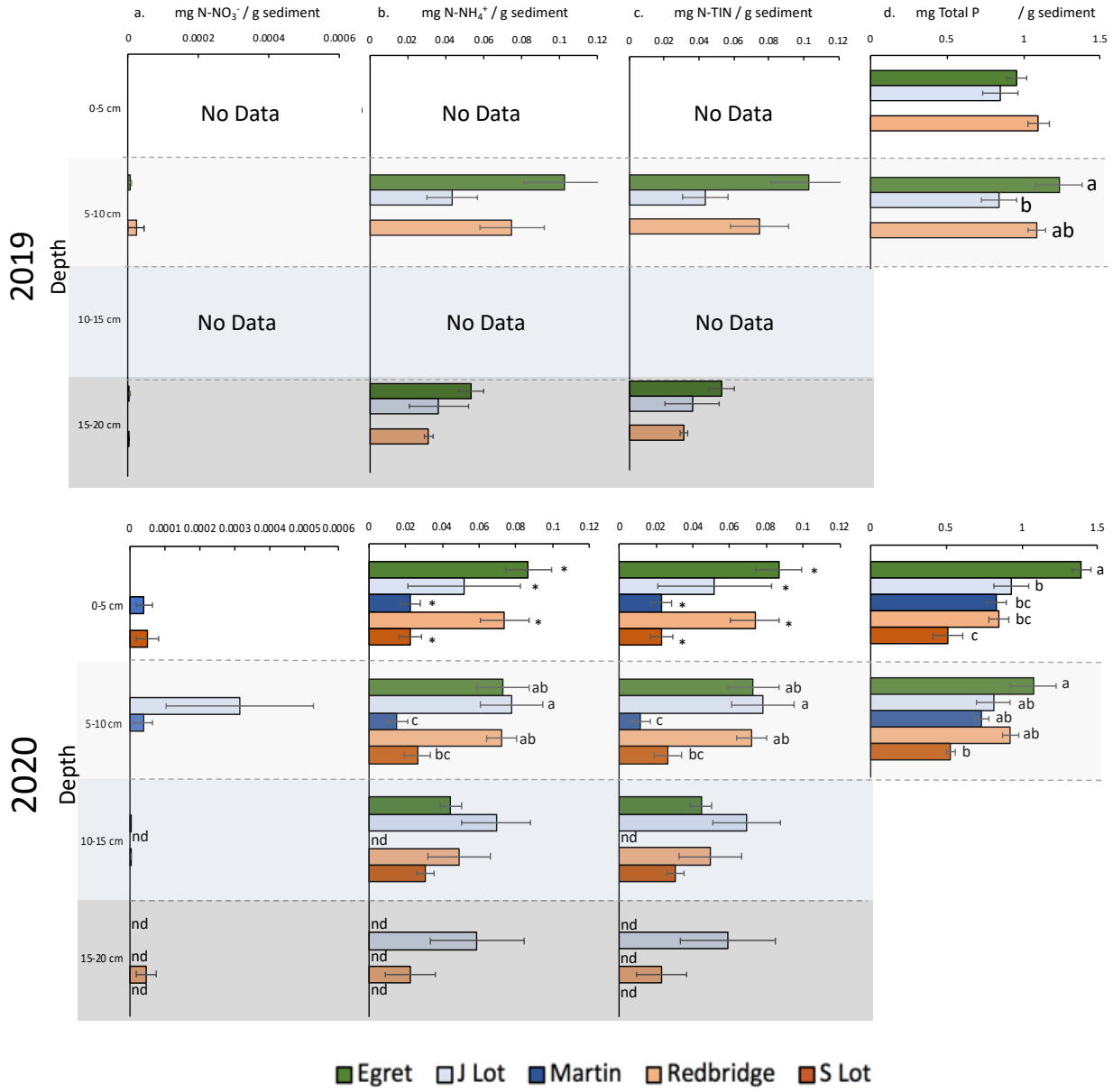

Figure 5. Sediment nutrient concentrations (avg ± SE, n = 4-5) including NO_3^- , NH_4^{3+}, TIN and TP from sediment collected on September 18th, 2019 and August 27th, 2020. One-way ANOVAs were applied to each depth and year separately. Tukey HSD results are shown. In 2019, TP 5-10 was found to be significant ($F_{2,11} = 5.7$, $p = .02$). In 2020, NH_4^{3+} 0-5 and 5-10 ($F_{4,15} = 3.1$, $p = .046$; $F_{4,15} = 5.9$, $p = .0053$), TIN 0-5 and 5-10 ($F_{4,15} = 3.1$, $p = .046$; $F_{4,15} = 7.5$, $p = .0016$), TP 0-5 and 5-10 ($F_{4,15} = 20$, $p < .0001$; $F_{4,15} = 4.2$, $p = .01$) were found to be significant. * indicates significant ANOVA but no differences detected by Tukey HSD.

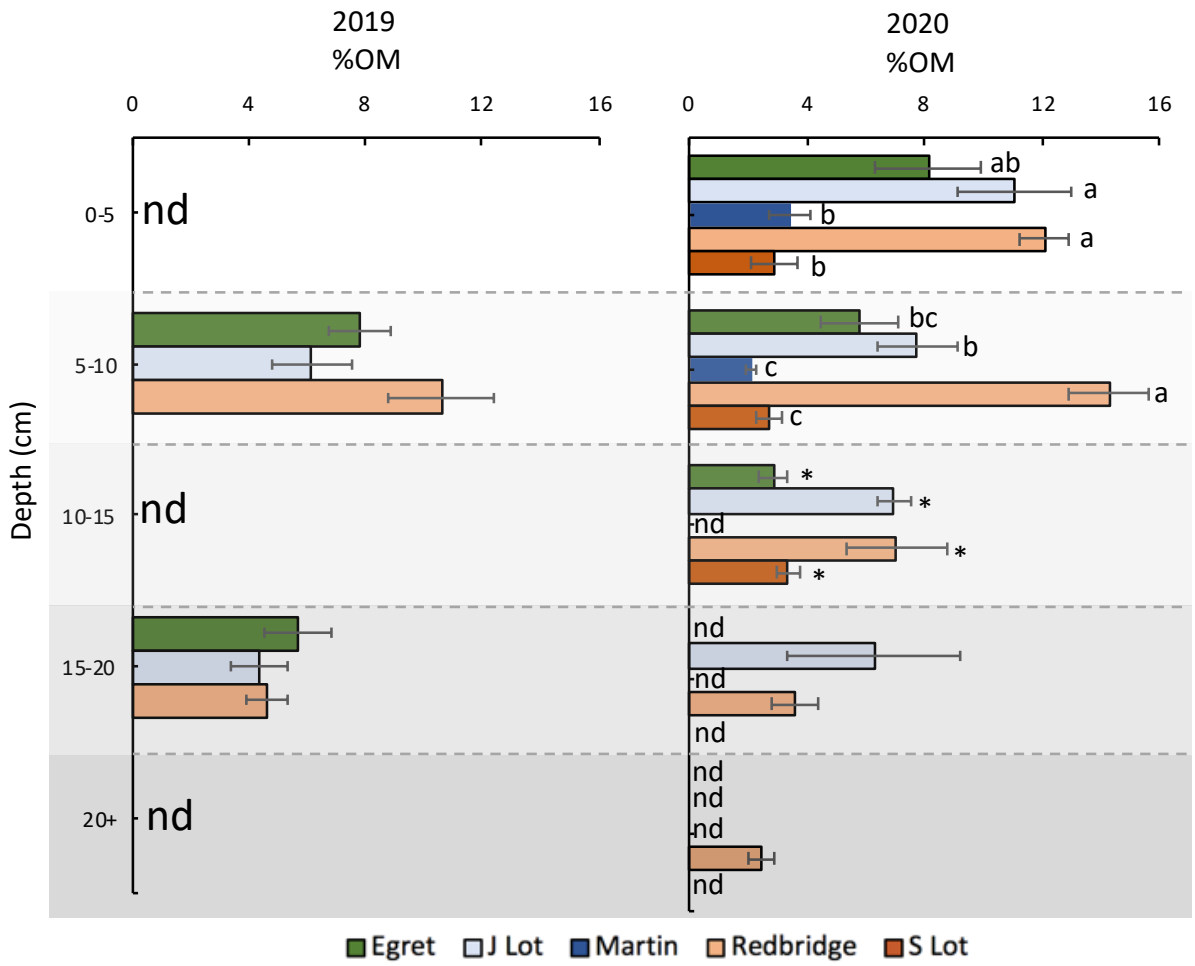

Figure 6. % OM (average ± SE, n = 4-5) for sediment collected on September 18th, 2019 and August 27th, 2020. One-way ANOVAs for each depth profile were run and only 0-5 cm ($F_{4,15} = 10.3$, $p < .001$), 5-10 cm ($F_{4,15} = 21.2$, $p < .0001$), and 10-15 cm ($F_{3,10} = 4.17$, $p < .037$) from 2020 were statistically significant. Tukey HSD test results are depicted. * indicates significance but with no differences detected by the Tukey HSD test.

Table 4. Summer ebullition data (June 21st – September 21st; n = 6-10) in mg CH_4 m^{-2} d^{-1} with Kruskal Wallis test results and Fisher's LSD groupings.

	Pond	N	Min	P10	Mean	Median	P90	Max	Group	*H*	*p*
2019	Egret	160	0.0303	18.5	290	257	572	1180	b	78.6	**< .0001**
	J Lot	204	0	11.0	234	170	572	1120	c		
	Nightfrost	160	0.243	16.6	433	351	895	4100	ab		
	Redbridge	158	0.0482	71.9	422	340	864	1710	a		
	Tinker	144	0.0272	1.55	210	133	554	915	c		
	Overall	826	0	10.8	315	247	680	4100	---		
2020	D Lot	107	0.150	58.8	264	217	559	835	b	288	**< .0001**
	Egret	119	36.7	132	416	359	745	1290	a		
	J Lot	118	0.00107	2.47	218	152	511	1610	c		
	Martin	105	0	0.0130	17.5	0.296	28.4	391	d		
	Redbridge	120	6.09	111	547	380	1230	3530	a		
	S Lot	120	16.3	72.2	343	323	619	1130	ab		
	Overall	689	0	0.846	308	221	665	3530	---		
Across Years	D Lot	107	0.150	58.8	264	217	559	835	bc	363	**< .0001**
	Egret	279	0.0303	70.9	344	305	659	1290	ab		
	J Lot	322	0	5.67	228	164	551	1610	c		
	Martin	105	0	0.0130	17.5	0.296	28.4	391	d		
	Nightfrost	160	0.243	16.6	433	351	895	4100	a		
	Redbridge	278	0.0482	106	476	350	919	3530	a		
	S Lot	120	16.3	72.2	343	323	619	1130	ab		
	Tinker	144	0.0272	1.55	210	133	554	915	c		
	Overall	1515	0	3.93	312	239	674	4100	---		

Table 5. Autumn ebullition data (September 22nd – October 30th; n = 6-10) in mg CH_4 m^{-2} d^{-1} with Kruskal Wallis test results and Fisher's LSD groupings.

		N	Min	P10	Mean	Median	P90	Max	Group	*H*	*p*
2019	Egret	52	0	0.00284	77.0	8.53	226	1080	b	35.8	**< .0001**
	J Lot	66	0	0.0174	33.4	1.56	130	288	b		
	Nightfrost	----	----	----	----	----	----	----	----		
	Redbridge	64	0.166	0.935	134	103.5	340	632	a		
	Tinker	62	0	0.0190	44.3	3.65	147	351	b		
	Overall	244	0	0.0321	71.8	13.5	225	1080	---		
2020	D Lot	30	1.01	7.54	73.0	44.1	186	460	ab	83.9	**< .0001**
	Egret	33	0.00208	0.0510	91.0	17.4	224	609	bc		
	J Lot	35	0.0420	0.104	43.7	13.1	124	320	c		
	Martin	33	0.00521	0.00728	0.747	0.0430	1.22	16	d		
	Redbridge	36	0.0256	3.47	117	61.4	370	729	ab		
	S Lot	34	7.00	15.3	170	70.7	362	1500	a		
	Overall	201	0.00208	0.0393	83.4	21.1	217	1500	---		
Across Years	D Lot	30	1.01	7.54	73.0	44.1	186	460	ab	118	**< .0001**
	Egret	85	0	0.0200	82.4	9.89	233	1080	bc		
	J Lot	101	0	0.0420	37.0	6.79	130	320	c		
	Martin	33	0.00521	0.00728	0.747	0.0430	1.22	16.4	d		
	Nightfrost	----	----	----	----	----	----	----	----		
	Redbridge	100	0.0256	1.21	128	87.5	354	729	a		
	S Lot	34	7.00	15.3	170	70.7	362	1500	a		
	Tinker	62	0	0.0190	44.3	3.65	147	351	c		
	Overall	445	0	0.0361	77.1	17.5	220	1500			

Table 6. Ebullition data (n = 6-10) in mg CH_4 m^{-2} d^{-1}across months with Kruskal Wallis test results and Fisher's LSD groupings. Nightfrost was omitted from the data since it was not sampled through the autumn.

		N	Min	P10	Mean	Median	P90	Max	Group	*H*	*p*
2019	June	127	3.17	70.6	277	223	606	1220	a	331	**< .0001**
	July	275	0.0272	39.4	353	287	741	1710	a		
	August	232	4.89E-03	25.6	286	254	607	928	a		
	September	142	2.30E-05	0.146	96.0	46.0	274	481	b		
	October	196	0	0.0167	60.7	3.88	201	1080	c		
2020	June	----	----	----	----	----	----	----	----	184	**< .0001**
	July	166	9.96E-03	0.283	373	326	782	1610	a		
	August	352	0	2.16	326	249	663	3530	a		
	September	239	1.69E-05	0.285	198	120	480	2120	b		
	October	133	2.08E-03	0.0203	36.5	15.3	104	242	c		
Across Years	June	139	3.17	71.2	278	223	593	1220	b	553	**< .0001**
	July	512	0.00996	17.2	386	326	771	4100	a		
	August	637	0	9.69	322	265	658	3530	b		
	September	413	1.697E-05	0.206	157	96.5	384	2120	c		
	October	329	0	0.0195	50.9	9.79	163	1080	d		

Table 7. Two tables of Kendall rank correlations between ebullition and other collected variables. τ indicates whether there is a positive or negative correlation. τ values greater than or equal to |0.5| were considered to have a strong correlation, between |0.3| and |0.5| were considered moderate correlations, between |0.1| and |0.3| were weak correlations and any τ value below |0.1| were considered very weak (Cohen, 2013). Where $p > .05$, correlations were nonsignificant. Significant *p* values are bolded.

	Water Temperature		Dissolved Oxygen		Conductivity		Water Depth		Δ Water Depth		Precipitation	
	τ	*p*	τ	*p*	τ	*p*	τ	*p*	τ	*p*	τ	*p*
D Lot	.396	**< .0001**	-.164	**.0054**	.133	**.025**	-.149	**.012**	-.286	**< .0001**	-.0955	.13
Egret	.329	**< .0001**	-.372	**< .0001**	.362	**< .0001**	.0760	.17	-.0562	0.323	-.159	**< .0001**
J Lot	.415	**< .0001**	-.0256	.44	.245	**< .0001**	-.235	**< .0001**	.0825	0.1535	-.0821	**.016**
Martin	.240	**< .0001**	-.0652	.28	.281	**< .0001**	-.101	.083	.240	**.0001**	-.140	**.027**
Nightfrost	.187	**< .001**	-.159	**.0032**	.298	**< .0001**	----	----	----	----	-.119	**.034**
Redbridge	.375	**< .0001**	.0117	.74	.278	**< .0001**	.200	**< .001**	.274	**< .0001**	-.102	**.0064**
S Lot	.324	**< .0001**	-.138	.89	.225	**< .0001**	.271	**< .0001**	.207	**< .001**	-.258	**< .0001**
Tinker	.237	**< .0001**	-.324	**< .0001**	.241	**< .0001**	----	----	----	----	-.0448	.38
Overall	.241	**< .0001**	-.0627	**< .0001**	.183	**< .0001**	-.259	**< .0001**	.0355	.13	-.102	**< .0001**

	Air Temperature		Avg. Atmospheric Pressure		Min. Atmospheric Pressure		Max. Atmospheric Pressure	
	τ	*p*	τ	*p*	τ	*p*	τ	*p*
D Lot	.431	**<.0001**	-.181	**<.002**	.0251	.67	-.323	**< .0001**
Egret	.375	**<.0001**	-.156	**<.0001**	.0729	**.034**	-.272	**< .0001**
J Lot	.363	**<.0001**	-.231	**<.0001**	-.0351	.27	-.288	**< .0001**
Martin	.216	**<.001**	-.0766	.19	.0477	.42	-.157	**.0076**
Nightfrost*	.320	**<.0001**	-.221	**<.0001**	.0435	.42	-.312	**< .0001**
Redbridge	.390	**<.0001**	-.143	**<.0001**	.0851	**.015**	-.261	**< .0001**
S Lot	.323	**<.0001**	-.0767	0.165	.110	**.048**	-.257	**< .0001**
Tinker	.327	**<.0001**	-.218	**<.0001**	-.00356	.94	-.237	**< .0001**
Overall	.320	**<.0001**	-.148	**<.0001**	.0435	**.0039**	-.233	**< .0001**

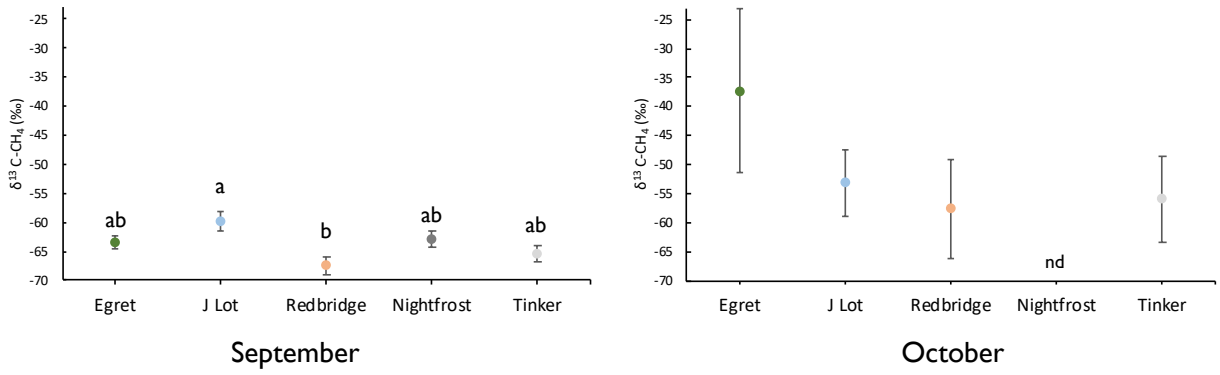

Figure 7. Composition of δ^{13}C-CH_4 (%) from ebullitive flux (Sept. 16th and Oct. 25th 2019, avg ± SE, n=4-8). One-way ANOVAs indicated significant differences amongst ponds in September ($F_{4,28} = 3.54$, $p = .02$) and between months ($F_{1,41} = 5.34$, $p = .002$). Tukey HSD results are depicted.

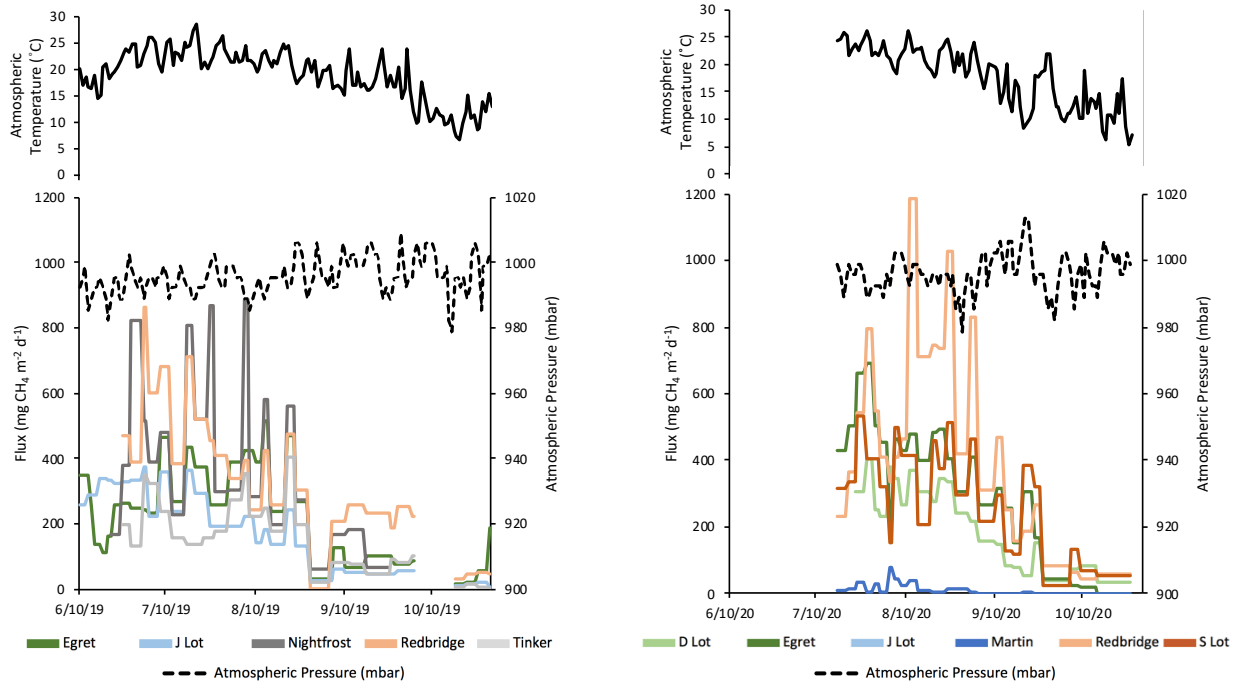

Figure 8. Plots of average ebullitive flux (n = 6-10) over the 2019 and 2020 field seasons. Daily data of atmospheric pressure and air temperature were laid overhead to illustrate how ebullition was related to changes in pressure and temperature.

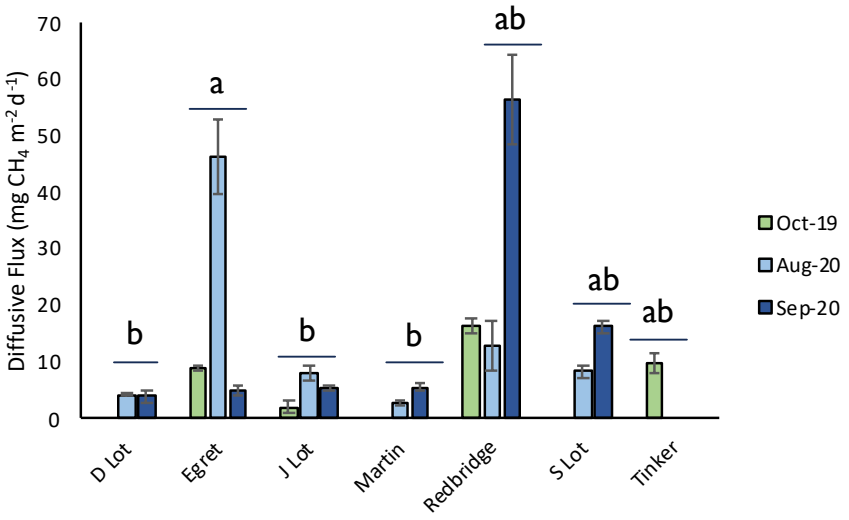

Figure 9. Diffusive flux data from the three sampling dates (average ± SE, n = 4). One-way ANOVA results indicate differences amongst ponds ($F_{7,52} = 3.79$, $p = .003$) and Tukey HSD results are shown.

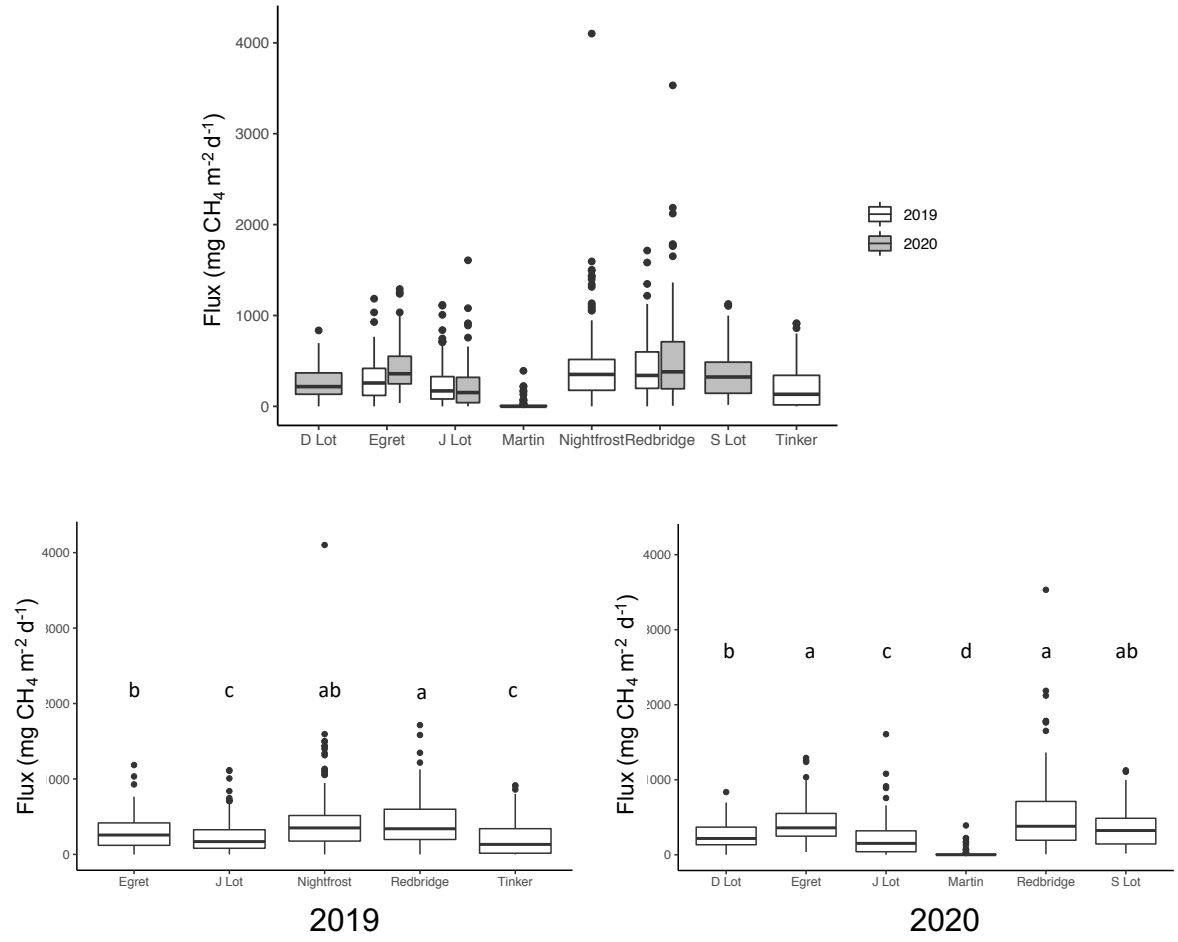

Figure 10. Box and whiskers plots for **summer** ebullition. The line within each box represents the median, boxes represent the interquartile range, the vertical lines represent the spread to the minimum and maximum, and the circles represent the outliers. The top plot includes both years sampled. The bottom plots show the same data but with the years separated, with groups determined by Fisher's LSD test after significance was found with the Kruskal-Wallis test ($p < .0001$).

Table 8. Linear regression results for average values amongst ponds for 2019, 2020 and combined years. Included are the *F* statistic, the adjusted R^2 and the *p* value. Values associated with a significant *p* value are bolded.

		2019			2020			Years Combined		
		F	R^2	*p*	*F*	R^2	*p*	*F*	R^2	*p*
Ebullition~	Diffusion	2.6	.35	.24	**8.0**	**.58**	**.047**	**8.0**	**.54**	**.037**
	Production	6.9	.74	.23	2.8	.31	.19	0.24	-.23	.65
	Oxidation	0.36	-.46	.65	2.2	.23	0.23	0.53	-.013	.52
	Temperature	2.4	.32	.26	0.16	-.19	.70	0.21	-.15	.67
	DO	0.021	-.48	.89	0.28	-.16	.62	1.8	.12	.24
	Conductivity	.062	-.45	.82	.23	-.18	.65	.72	-.048	.43
	Chl *a*		----nd----		4.1	.38	.11		----nd----	
	^{13}C	0.49	-.15	.53		----nd----			----nd----	
	Depth	0.14	-.39	.73	0.28	-.16	.62	**32**	**.84**	**.0024**
	OM 0-5		----nd----		1.5	.11	.31		----nd----	
	Sediment TIN 0-5		----nd----		47	-.15	.54		----nd----	
	Sediment TP 0-5	1.8	.30	.40	0.16	-.26	.71	0.008	-.33	.93
	Water TIN	**780**	**.99**	**.0012**	1.80	.13	.25	1.6	.097	.25
	Water PO_4^{3-}	.39	-.25	.59	.028	-.24	.87	0.49	-.093	.51
Production~	Oxidation	.032	-.93	.89	**26**	**.86**	**.015**	5.1	.50	0.10
	OM 0-5		----nd----		**35**	**.90**	**.0096**		----nd----	

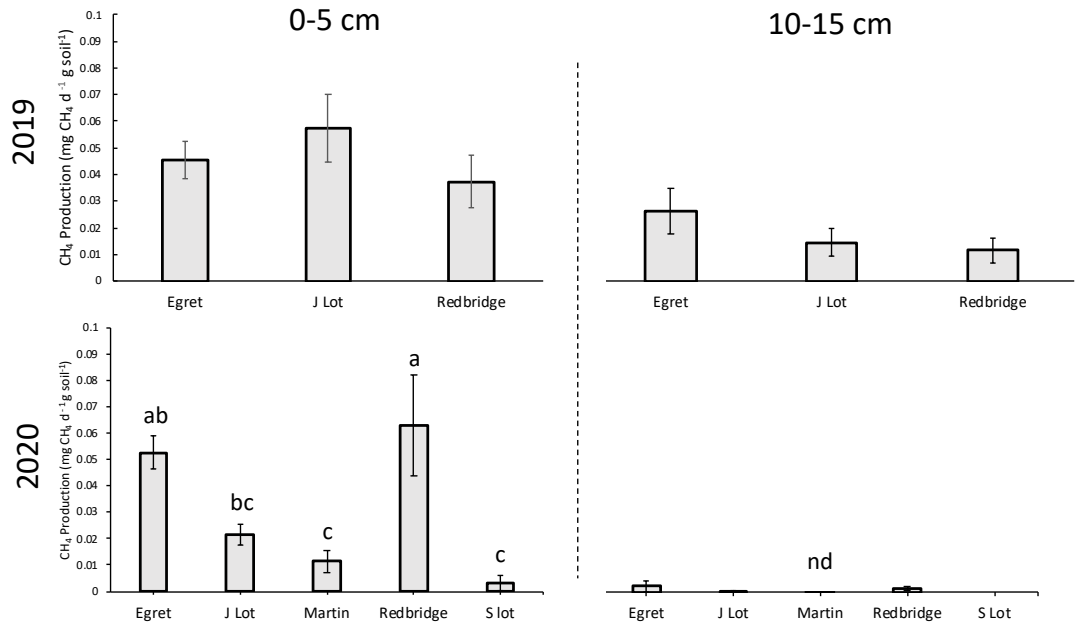

Figure 11. CH_4 production data from sediment cores in 2019 and 2020 (average ± SE, n = 4-5) for 0 to 5 cm and 10 to 15 cm depth profiles. One-way ANOVA results suggest 0-5cm 2020 production were different amongst ponds ($F_{4,19}$ =7.65, p = .001). Tukey HSD groups are shown.

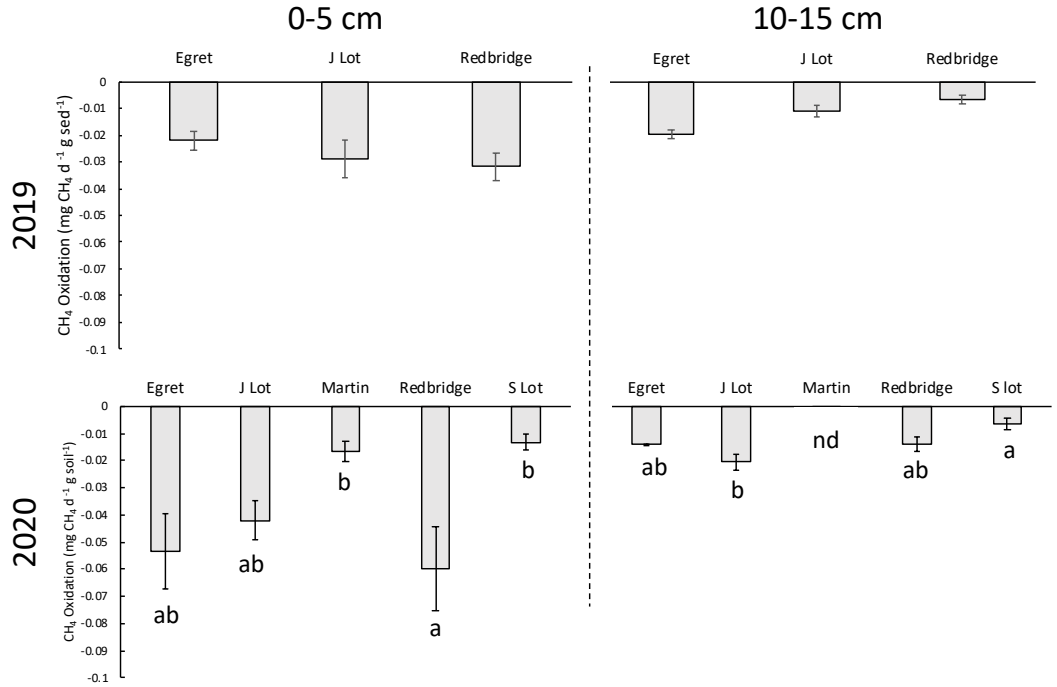

Figure 12. CH_4 oxidation data for sediment cores from 2019 and 2020, (average ± SE, n = 4) for 0 to 5 cm and 10 to 15 cm depth profiles. Both depth profiles had significant differences amongst ponds in 2020 identified by one-way ANOVAs (0-5: $F_{4,20}$ =4.97, p = .01; 10-15: $F_{3,16}$ =5.16, p = 0.02). Tukey HSD groups are shown.

Table 9. A compilation of all studies that have looked at CH_4 emissions from "stormwater wet/retention" or "urban" ponds.

	Gorsky	Grinham	Herrero Ortega	Martinez-Cruz	Peacock	van Bergen	This study
Location	Virginia, US	Queensland, AU	Berlin, DE	Mexico City, MX	Uppland, SE	Gelderland, NL	New York, US
Latitude	32.27° N	22.58° S	52.52° N	19.43° N	59.86° N	51.78° N	43.06° N
Sampling Months	June to Aug.	Aug to Sept	Feb. to Oct.	Jan - Feb, May - June, Aug - Sept	May to June	July to May	June to Oct.
CH_4 flux (mg CH_4 m^{-2} d^{-1})	362	129	503	20	30.3	120	268